Doctoral Thesis

博士論文

Research on Multicarrier CDMA Schemes with Interference Free Performance Using ZCZ Code in Large Delay Spread

超遅延波に対して干渉の無いマルチキャリア ZCZ-CDMA 方式に関する研究

November, 2014

AINIWAN ABUDOUKEREMU

Graduate School of Science and Engineering

Yamaguchi University, Japan

Abstract

A wireless communication technology that allows multiple users to communicate in real time is strongly required to support various needs such as high performance remote control systems to simultaneously move many mobile units like robots and vehicles and wireless network systems to dynamically link mobile units.

Direct sequence code division multiple access (DS-CDMA) with a quasi-synchronous technique and a set of orthogonal sequences with a zero correlation zone (ZCZ code), which is called DS-ZCZ-CDMA collectively, achieves multiple access interference (MAI) from adjacent users and inter symbol interference (ISI) due to multi-path free performance and synchronization capability with fast frame acquisition within one chip delay spread. Moreover, a block spreading technique is applied to the DS-CDMA, which uses ZCZ code and MMSE RAKE receiver utilizing the pilot sequence for channel estimation to remove the MAI called BC-DS-ZCZ-CDMA.

On the other hand, multicarrier CDMA (MC-CDMA) with frequency domain spreading and multicarrier direct sequence CDMA (MC-DS-CDMA) with time domain spreading based on a combination of the orthogonal frequency division multiplexing (OFDM) and DS-CDMA with the advantages of effective frequency utilization and high tolerance to multi-path fading has been proposed. Furthermore, MC-CDMA using ZCZ code has been discussed. However, in high data rate transmission with large delay spread, MAI, ISI and inter carrier interference (ICI) cause the system performance degradation.

In order to remove these interferences, this dissertation proposes a new MC-CDMA scheme without the MAI and ICI over a very large delay spread channel. The proposed scheme can be characterized by a block coding technique using a set of sequences with ZCZ code and the

minimum mean square error (MMSE) RAKE receiver utilizing the pilot sequence for channel estimation to remove MAI and ICI, and to reduce the influence of the ISI, respectively. The proposed scheme does not need frequency domain equalization technique. In order to demonstrate the improved bit error rate (BER) performance of the proposed scheme comparing with conventional MC-CDMA under the same condition in large delay spread, a computer simulation is applied.

It is clarified that proposed scheme using ZCZ code with the maximum family size possesses good BER performance for large delay spread dose not exceed the block size. For the conventional schemes using ZCZ code, it has been shown that some are affected by the interferences even in the case of one chip delay spread, and in others, the delay length without MAI depends on the size of zero correlation zone, that is, the family size of sequences decreases. Thus, there is a trade-off of the BER performance and the number of users in those conventional schemes. In the proposed scheme, the block size does not almost affect the system performance if block size is longer than the length of large delay spread. If code length is large, even if code length exceeds length of large delay spread, the performance can be maintained.

Contents

List of Abbreviations

2G	second generation
3G	third generation
4G	fourth generation
LTE	long term evolution
TDMA	time division multiple access
FDMA	frequency division multiple access
CDMA	code division multiple access
DS-CDMA	direct sequence code division multiple access
FH-CDMA	frequency hopping code division multiple access
OFDM	orthogonal frequency division multiplexing
MC-CDMA	multicarrie code division multiple access
MC-DS-CDMA	multicarrie direct sequence code division multiple access
BER	bit error ratio
E_b/N_o	per bit energy-to-noise ratio
MMSE	minimum mean square error
ZCZ	zero correlation zone
GI	guard interval
AWGN	additive white Gaussian noise
ISI	inter symbol interference
ICI	inter carrier interference
MAI	multiple access interference
DFT	discrete Fourier transform
IDFT	inverse discrete Fourier transform
PDF	probability density function
RMS	root mean square
dB	decibel
LOS	line-of-sight
NLOS	non line-of-sight

ASK	amplitude shift keying
PSK	phase shift keying
BPSK	binary phase shift keying
QPSK	quadrature phase shift keying
16QAM	16-quadrature amplitude modulation
BC	block coding
P/S	parallel-to-serial
S/P	serial-to-parallel
GO	general orthogonal code
EO	E-sequences
GZCZ	ZCZ code derived from GO code
EZCZ	ZCZ code derived from EO code

Chapter1

Introduction

In this chapter, the background and purpose of this research is described. Then, the layout of the dissertation is presented.

1.1 Background and Research Purpose

A wireless communication technology that allows multiple users to communicate in real time is strongly required to support various needs such as high performance remote control systems to simultaneously move many mobile units like robots and vehicles and wireless network systems to dynamically link mobile units.

As an effective technique, code division multiple access (CDMA) schemes that multiple users can communicate over the same frequency band simultaneously are considered [1]- [3]. There are the direct sequence CDMA (DS-CDMA) and multicarrier CDMA (MC-CDMA) including multicarrier direct sequence CDMA (MC-DS-CDMA) as important CDMA schemes with the advantages of effective frequency utilization and high tolerance to multipath fading [4]- [6].

In general, DS-CDMA that original data symbols are spread by a high-rate sequence in time domain, has been adopted to synchronous and asynchronous communications, which have been adopted to downlink and uplink for third generation (3G) cell phones, respectively [7]- [10]. The downlink uses an orthogonal code corresponding to a Hadamard matrix referred to as a spreading sequence set to cancel the inter symbol interference (ISI) due to multipath fading and multiple access inter-

ference (MAI) from adjacent multiple users [11]- [14]. The uplink uses a spreading code with good auto and cross-correlation properties such as a pseudo-random (PN) sequence set and the Gold sequence set, etc. to suppress ISI and MAI.

DS-CDMA with a quasi-synchronous technique and a zero correlation zone (ZCZ) code including a complementary code, which is called DS-ZCZ-CDMA collectively, achieves ISI and MAI free performance and synchronization capability with fast frame acquisition [22]- [27]. DS-ZCZ-CDMA can be applicable flexibly in not only Infrastructure mode but also Ad-hoc mode [28], because two-way communication without MAI is possible over the same frequency channel. On a large delay spread channel caused by high data rate transmission, the influence of MAI, ISI and synchronization gap deteriorates the communication performance. As a solution, DS-ZCZ-CDMA based on a block spreading technique called DS-BC-ZCZ-CDMA has been proposed successfully, which uses ZCZ code and the minimum mean square error (MMSE) RAKE receiver utilizing the pilot sequence for channel estimation [29]- [33].

On the other hand, MC-CDMA based on a combination of the orthogonal frequency division multiplexing (OFDM) using the Fourier transform technique with DS-CDMA has been adapted to synchronous communication, that an original data symbol is spread by a sequence in an orthogonal code over different subcarriers in frequency domain [34]- [37]. MC-DS-CDMA with spreading in time domain, that an orignal data symbol multiplied by a sequence is allocated to each subcarrier, has been discussed [41], [42]. In general, the bit error rate (BER) performance of MC-DS-CDMA is worse than that of MC-CDMA, since the influence of ISI and inter carrier interference (ICI) due to multipath fading is large. It is known that the required frequency band of MC-CDMA and MC-DS-CDMA is smaller almost half than that of DS-CDMA [5], [38], [60]. However, in high data rate transmission, the system performance is still limited by MAI, ISI and ICI.

In order to remove these interferences, MC-CDMA and MC-DS-CDMA using ZCZ code have been discussed [43]- [48]. However, some are affected by the interferences even in the case of one chip delay spread, and in others the delay length without MAI depends on the size of zero correlation zone, that is, the family size of sequences decreases. Thus, there is a trade-off of the BER performance and the number of

multiple users in the above conventional CDMA schemes.

1.2 Overview of this Dissertation

The dissertation proposes a novel multicarrier CDMA scheme without interferences over a multipath Rayleigh fading channel with large delay spread, which can be characterized by a block coding technique using a ZCZ code with low correlation property and the MMSE RAKE receiver utilizing the pilot sequence for channel estimation to remove MAI and ICI, and to reduce the ISI, respectively.

The dissertation consists of six chapters. The respective contents of the succeeding chapters are follows:

Chapter 2 presents some necessary fundamental knowledge of digital communication schemes to help understand the main intention of the research. The basic structure of the wireless communication channels and modulation schemes are introduced. An intensive explanation is given to singlecarrier and multicarrier CDMA schemes including DS-CDMA, OFDM and MC-CDMA.

In chapter 3, MC-ZCZ-CDMA is illustrated. A ZCZ code with low correlation properties is given and its orthogonality for time domain and frequency domain on the Fourier transform is mathematically verified and clarified for one chip delay. A general DS-ZCZ-CDMA and a MAI-free BC-DS-ZCZ-CDMA schemes are introduced and their problems for high data rate transmission are depicted. A MC-ZCZ-CDMA scheme without GI technique is presented and its problem is depicted.

In chapter 4, to sole above problems, a MC-ZCZ-CDMA in large delay spread is investigated. At first, a basic MC-ZCZ-CDMA with guard interval (GI) is given to combat these interferences by using the correlation properties of ZCZ code for one chip delay even the transmitted data symbols increases. Then, a novel MC-ZCZ-CDMA scheme without the interferences called BC-MC-ZCZ-CDMA based on the above scheme is proposed. BC-MC-ZCZ-CDMA is characterized by use of a block coding (BC) technique using ZCZ code to remove MAI and ICI in very large delay spread, and the RAKE receiver utilizing the pilot sequence for channel estimation to utilize a delay wave and to reduce ISI. The length of delay chips is related to only block size and does not depend on the size of the zero correlation zone. It does

not have the trade-off mentioned above, and does not need the frequency domain equalization technique [34] which has been used in multicarrier communications generally, since MAI and ICI are free.

In order to demonstrate the improved BER performance of the proposed scheme by comparing with conventional schemes in a large delay spread channel, a computer simulation is applied in chapter 5 and these schemes's performances are analized. Chapter 6 concludes the dissertation and gives topics for further study.

Chapter2

Fundamentals of Communication Systems

In this chapter, firstly, the fundamentals of digital communication systems are reviewed. Next, the basic structure of wireless communication channels is introduced. Additive white Guassian noise (AWGN) and multipath fading channel with a large delay spread are presented. Then, different data modulation schemes are presented. Finally, an intensive explanation is given to singlecarrier and multicarrier schemes including DS-CDMA, OFDM and MC-CDMA.

2.1 Digital Communication Systems

Spread spectrum communications have long been used in military systems. The distinguishing feature of spread spectrum communications is that the transmission bandwidth is significantly higher than that required by the information rate, resulting in the spread terminology. Typically, a pseudo-random code is used to spread the information signal to the allocated frequency bandwidth [1].

CDMA as a multiple access scheme has advantages and disadvantages over the more traditionally employed frequency division multiple access (FDMA) and time division multiple access (TDMA) [2], [3]. If all three multiple access schemes are compared under the hypothetical conditions of a Gaussian channel and all the users are perfectly orthogonal to each other, then all three schemes are equivalent with re-

spect to Shannon ' s channel capacity. However, mobile communications are usually conducted over radio channels that are more hostile than the ideal Gaussian channel and these radio channels lead to performance differences amongst the three multiple access schemes. In comparison to FDMA and TDMA schemes, CDMA scheme suffers more severe MAI due to the often imperfect cross-correlation properties of the spreading codes used. The user signals in FDMA and TDMA are inherently orthogonal to each other due to the orthogonal frequency and time slots used. However, FDMA and TDMA are primarily dependent on the availability of bandwidth, which is a costly resource, and the capacities of both these schemes are therefore bandwidth-limited. However, the CDMA is only interference-limited.

Techniques differ from each other in the way that the information signal is transformed to produce a high-bandwidth spread signal. In Direct Sequence CDMA (DS-CDMA), a pseudorandom sequence having a higher bandwidth than the information signal is used to modulate the information signal directly. The resultant signal has a significantly higher bandwidth than the original signal [7]. In Frequency Hopping CDMA (FH-CDMA), the transmission bandwidth is divided into frequency sub-bands, where the bandwidth of each sub-band is equal to the bandwidth of the information signal. A pseudo-random code is then used to select the subband, in which the information signal is transmitted and this sub-band changes periodically according to the code [4].

In second generation (2G) DS-CDMA scheme, specifically in the Qualcomm IS-95 CDMA standard, the MAI is treated as noise. Then, the DS-CDMA has been adopted to synchronous and asynchronous communications, which have been adopted to downlink and uplink for third generation (3G) cell phones, respectively [7], [8], [11]. The downlink uses an orthogonal code corresponding to a Hadamard matrix referred to as a spreading sequence set to cancel the inter symbol interference (ISI) due to multipath fading and multiple access interference (MAI) from adjacent multiple users. The uplink uses a spreading code with good auto and cross-correlation properties such as a pseudo-random sequence set and the Gold sequence set, etc. to suppress ISI and MAI [12]- [14].

Hybrid CDMA encompasses a group of techniques that combine two or more of the other schemes already described. One of these hybrid schemes is known as mul-

ticarrier CDMA. OFDM is a parallel data transmission scheme in which high data rates can be achieved by transmitting mutual orthogonal subcarriers [5], [6]. However, in OFDM, the ISI and ICI due to multipath induces the system performance degradation [57]- [59]. Thus, the performance degradation in OFDM is reduced by the insertion of guard interval (GI) and code synchronization is made easier by the extended symbol period engendered by the associated serial-to-parallel conversion proceeding the parallel transmission of low-rate subchannels. Recently, multicarrier CDMA schemes including MC-CDMA with frequency domain spreading and MC-DS-CDMA with time domain spreading based on the combination of CDMA and OFDM have attracted attention in the field of wireless communications. This is mainly due to the need to support high data rate services in wireless environment characterized by highly hostile radio channels. These signals can be efficiently modulated and demodulated using inverse discrete Fourier transform (IDFT) and discrete Fourier transform (DFT) techniques without substantially increasing the complexity of the transmitter and receiver [21], [60], [61]. These systems also exhibit the attractive feature of high spectral efficiency, since they can operate using a low Nyquist roll-off factor. Hence, OFDM can approach maximum bandwidth efficiency associated with Nyquist sampling. The combination of CDMA and OFDM can combat the effects of fading channels by spreading signals over several orthogonal subcarriers, and it provides high frequency diversity. This dissertation focuses on MC-CDMA scheme. Because it provides high frequency diversity and has ability to mitigate the ISI, ICI and MAI in a multipath Rayleigh fading channel with large delay spread.

2.2 Wireless Communication Channels

In recent years, wireless communications have experienced massive growth and commercial success [18]. However, in wireless communications, the radio channels are usually not amiable as the wired one. In wireless communication, multi-path fading is a common phenomenon that results in transmitted signals arriving the receiver by two or more paths [19]. As shown in Figure 2.1, when a signal is transmitted over a multipath propagation channel, it is subjected to reflection, refraction and

diffraction, as a result, causes errors and affects the quality of communications.

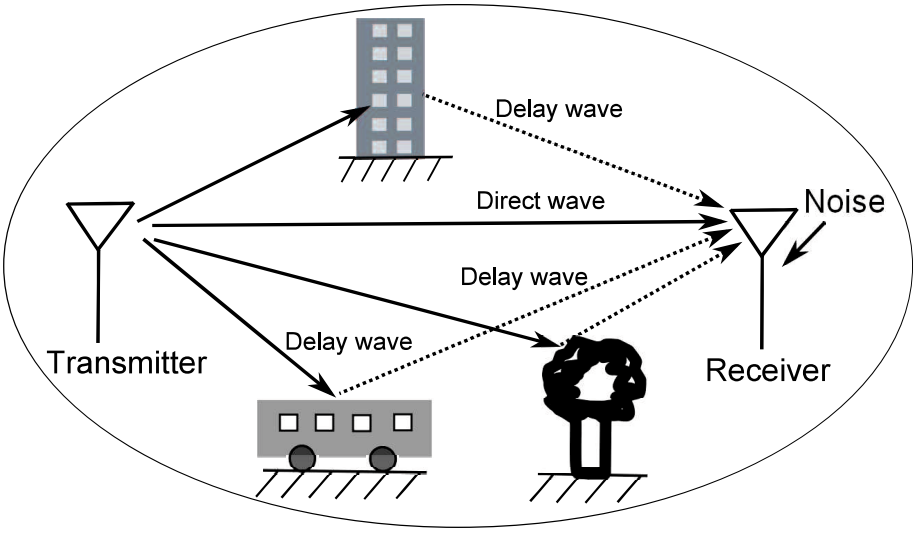

Figure 2.1: Wireless channel

2.2.1 AWGN

Additive white Gaussian noise (AWGN) is the statistically random radio noise characterized by a wide frequency range with regards to a signal in a communications channel. The randomness of AWGN in time domain will cause a transmitted symbol to be distorted such that the receiver interprets it as a different symbol in the modulation scheme. Under these circumstances, a given average level of AWGN introduces an average number of symbol errors at output of the receiver.

In communication channels, a basic model of AWGN is the set of assumptions that the noise is additive, i.e., the received signal equals the transmit signal plus some noise, where the noise is statistically independent of the signal, the noise is white, i.e, the power spectral density is flat. So, the autocorrelation of the noise in time domain is zero for any non-zero time offset and the noise samples have a Gaussian distribution as shown in Figures 2.2 and 2.3, respectively.

The probability density function (PDF) of Gaussian distribution is represented as

$$p(x) = \frac{1}{\sqrt{2\pi\sigma^2}} e^{-\frac{(x-\mu)^2}{2\sigma^2}}, \tag{2.1}$$

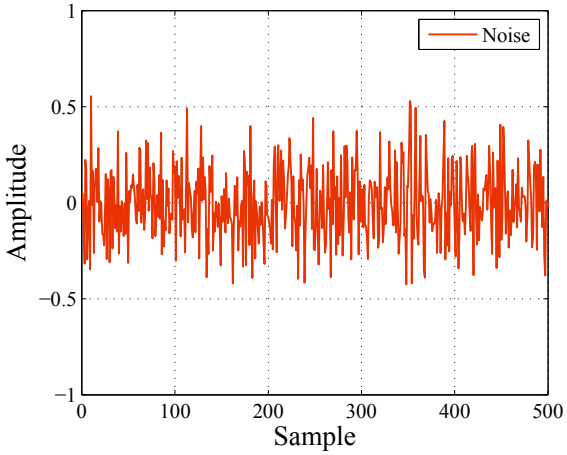

Figure 2.2: AWGN in time domain

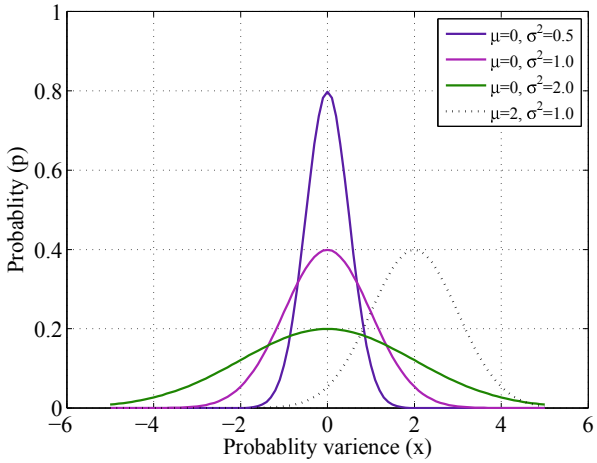

Figure 2.3: Gaussian distribution

where x is the amplitude of the received signal, μ is the average and σ^2 is the noise variance. In most case, $\mu = 0$ is assumed. As the noise power increases, the decision error probability becomes higher.

Per bit energy-to-noise ratio (E_b/N_0) is probably in the most common and well understood performance measure characteristic of a digital communication system. Most often this is measured at the output of the receiver and is thus directly related to the data detection process itself. E_b/N_0 is a term for the power ratio between a

signal and the background noise defined by

$$E_b/N_0 = \frac{P_s}{P_n} = \left(\frac{A}{\sigma}\right)^2, \tag{2.2}$$

where P_s is average signal power and P_n is average noise power. A and σ are root mean square (RMS) amplitude for signal and noise.

Since radio signals have a very large dynamic range, E_b/N_0 is usually expressed in terms of the logarithmic decibel (dB) scale as

$$(E_b/N_0)_{dB} = 10log_{10}\frac{P_s}{P_n} = 20log_{10}\frac{A}{\sigma}. \tag{2.3}$$

2.2.2 Multipath Fading

In wireless communications, fading is deviation of the attenuation affecting a signal over certain propagation media. In wireless systems, fading may either be due to multipath propagation, or due to shadowing from obstacles affecting the wave propagation. There are two kinks of fading such as Rician fading and Rayleigh fading [20] as shown in Figures 2.4(a) and (b), respectively.

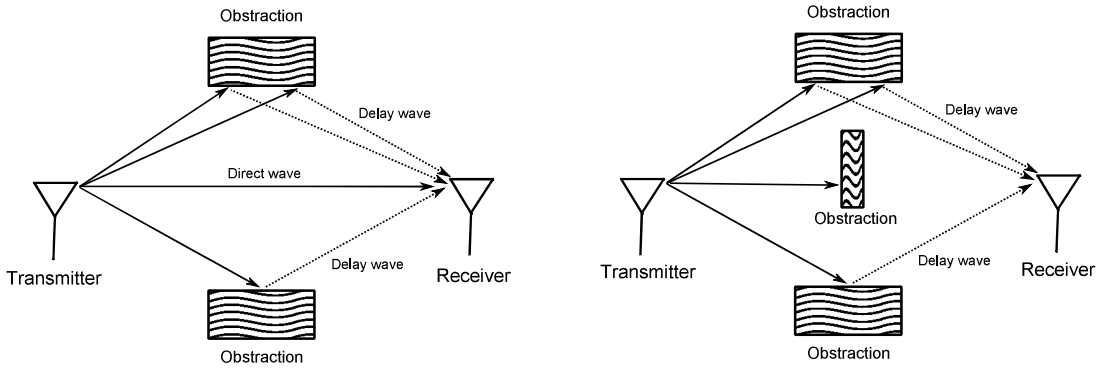

(a) LoS for Rician fading

(b) NLoS for Rayleigh fading

Figure 2.4: A basic model of Rician and Rayleigh fading

The former occurs when one of the paths, typically a line-of-sight (LOS) signal, is much stronger than the others. In Rician fading, the amplitude gain is characterized by a Rician distribution as shown in Figure 2.5. The PDF is expressed as

$$p(x) = \frac{x}{\sigma_x^2} e^{-\frac{(x^2-v^2)}{2\sigma_x^2}} I_0\left(\frac{xv}{\sigma_x^2}\right), \tag{2.4}$$

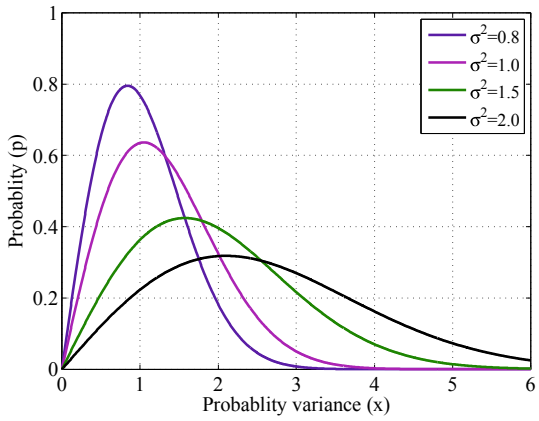

Figure 2.5: Rician probability density function

where v is the amplitude of a direct wave with $x \geq 0$ and $v \geq 0$, σ_x^2 is the average received power, and $I_0(.)$ is the modified Bessel function of the first kind and zeroth order, respectively.

On the other hand, Rayleigh fading is the specialized model for stochastic fading when there is no line-of-sight (NLOS) signal, and is sometimes considered as a special case of the more generalized concept of Rician fading. In Rayleigh fading, the amplitude gain is characterized by a distribution as shown in Figure 2.5. By Eq.(2.4), the PDF is expressed as

$$p(x) = \frac{x}{\sigma_x^2} e^{-\frac{(x^2+v^2)}{2\sigma_x^2}}. \tag{2.5}$$

As shown in Figure 2.4, in a Rayleigh fading, the received field intensity is considerably decreased due to the interference of a delay wave with the same intensity. On the other hand, the attenuation of the received field intensity in a Rician fading is lower than it of a Rayleigh fading due to a strong direct wave.

In Figure 2.6(a), flat fading occurs when the bandwidth of the transmitted signal B_S is less than the coherence bandwidth of the channel B_C, written as

$$B_S \leq B_C. \tag{2.6}$$

Equivalently if the symbol period of the signal T_S is more than the delay spread

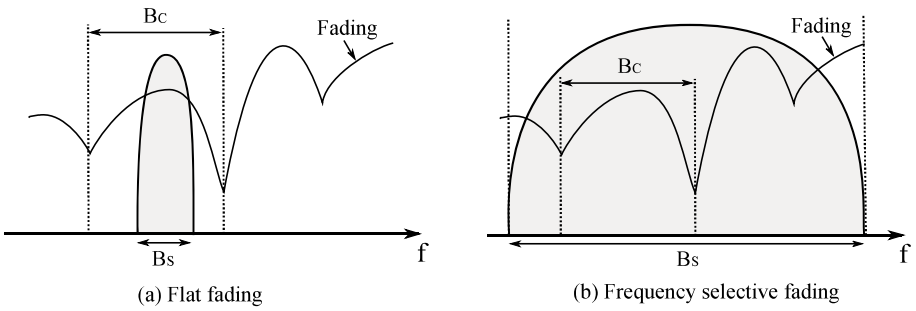

Figure 2.6: Flat and frequency selective fading

of the channel τ, written as

$$T_s \leq \tau. \tag{2.7}$$

And in such a case, mobile channel has a constant gain and linear phase response over its bandwidth.

On contrast, in Figure 2.6(b), frequency selective fading occurs when B_S is greater than B_C, written as

$$B_S \geq B_C. \tag{2.8}$$

Equivalently if T_S is more than τ, written as

$$T_s \geq \tau. \tag{2.9}$$

And in such a case, mobile channel has an unconstant gain and nonlinear phase response over its bandwidth. Finally, the system performance degrades by this kinds of fading channels.

In multi-path environments with frequency selective fading , the received radio signal from the transmitter consists of typically a direct signal, pulse reflections off objects such as building is impaired by a time delay and a level of a delay wave. Thus, this time-dispersive paths causes system performance degradation. A propagation channel consists of J distinct paths with different time delay chips . The channel impulse response $p^m(\tau, t)$ of the mth user is expressed as

$$p^m(\tau, t) = \sum_{j=0}^{J-1} p_j^m(t)\delta(\tau - \tau_j^m), \tag{2.10}$$

where $p_j^m(t)$ denotes the complex channel gain at time t, τ_j^m the time delay τ of the jth path of mth user, and $\delta(.)$ the delta function. The channel transfer function $H^m(f,t)$, which is the Fourier transform of $p^m(\tau,t)$, is written as

$$\begin{aligned} H^m(f,t) &= \int_0^\infty p^m(\tau,t)e^{-j2\pi f\tau_j^m}d\tau \\ &= \sum_{l=0}^{J-1} p_j^m(t)e^{-j2\pi f\tau_j^m}. \end{aligned} \tag{2.11}$$

Figure 2.7 shows the appearance of delay spread in multi-path Rayleigh fading channel. If the time delay spread $\tau_1 = \cdots = \tau_{J-1} = 0$, then the interference does

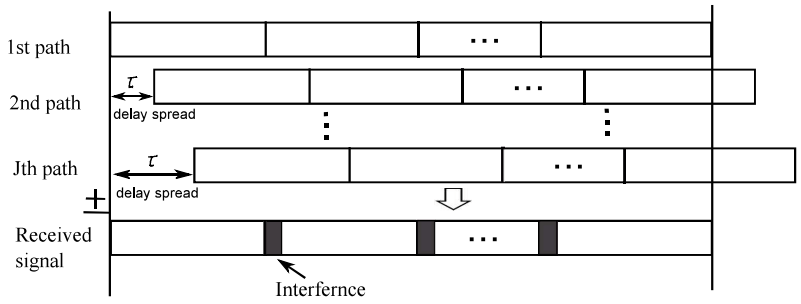

Figure 2.7: Delay spread in multipath Rayleigh fading channel

not occur. Contrarily, when a large delay spread exists, i.e., $\tau_j > 0$, the interference occurs and strongly influence system performance.

The propagation model of Eq.(2.10) and Figure 2.7 with large delay spread is shown in Figure 2.8,

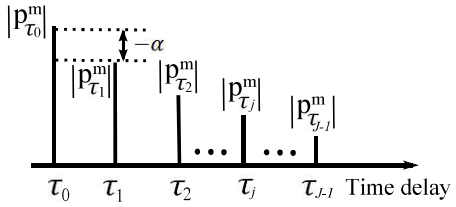

Figure 2.8: Propagation channel model

The average received signal levels of J delay paths are written as

$$\mathbf{p^m} = (p_{\tau_0}^m, p_{\tau_1}^m, \cdots, p_{\tau_j}^m, \cdots, p_{\tau_{J-1}}^m), \tag{2.12}$$

where $p_{\tau_j}\overline{p}_{\tau_j} = |p_{\tau_j}|^2$, $\overline{(.)}$ is the complex conjugate and τ_j denotes the length of the maximum delay spread of jth delay path with $\tau_0 = 0$ and $\tau_j - \tau_{j-1} \geq 1$, α is a decay

factor of the propagation channel defined by

$$\alpha = 10log_{10}(\frac{|p_{\tau_j}|^2}{|p_{\tau_{j+1}}|^2}). \tag{2.13}$$

If $\alpha = 0$ dB, it means the equivalent power delay profile. In this dissertation, two-path channel with $\alpha = 0$ is considered in computer simulation.

2.3 Modulation Schemes

Phase shift keying (PSK) is a method of digital communication in which the phase of a transmitted signal is varied to convey information [2], [16]. The mathematical representation of PSK modulated signal $x_c(t)$ can be written as

$$\begin{aligned} x_c(t) &= rcos(2\pi f_c t + \theta) \\ &= x_I(t)cos2\pi f_c t - x_Q(t)sin2\pi f_c t, \end{aligned} \tag{2.14}$$

with

$$r = \sqrt{x_I^2(t) + x_Q^2(t)}, \tag{2.15}$$

where x_I is the in-phase component, x_Q is the quadrature component and f_c is the frequency. The phase ϕ can be expressed by

$$\phi = cos^{-1}(\frac{x_Q(t)}{r}) \quad or \quad \phi = sin^{-1}\frac{x_I(t)}{r}. \tag{2.16}$$

By using famous Euler's equation $e^{j\theta} = cos\theta + jsin\theta$, Eq.(2.14) can be written as

$$x_c(t) = R[x_B(t)e^{j2\pi f_c t}], \tag{2.17}$$

where x_B is called the baseband equivalent signal and is given by

$$x_B(t) = x_I(t) + jx_Q(t). \tag{2.18}$$

Moreover, two orthogonal basis functions ϕ_1 and ϕ_2 is expressed by

$$\phi_1 = \sqrt{\frac{2}{T_s}}cos2\pi f_c t, \quad \phi_2 = -\sqrt{\frac{2}{T_s}}sin2\pi f_c t, \tag{2.19}$$

where T_s is the period of symbol.

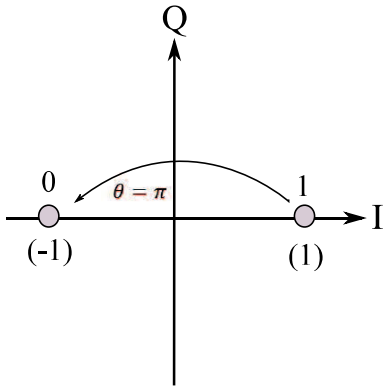

Figure 2.9: Constellation diagram of a BPSK

2.3.1 BPSK and QPSK

Binary phase shift keying (BPSK) is the simplest form of PSK. It is represented by two points on the constellation diagram as shown in Figure 2.9. Corresponding to each constellation point, the two possible digital passband signals, one of which is selected for transmission in each symbol interval, are given by

$$x_{c1} = Acos2\pi f_c t, \quad x_{c2} = -Asin2\pi f_c t, \tag{2.20}$$

where A is the amplitude with elements $1, -1$ of transmitting signal.

By using Eqs.(2.19) and (2.20), the projection of x_{c1} along the two axes in the constellation diagram is given by

$$x_{c1,\phi_1} = \int_{T_s}^{\infty} x_{c1}(t)\phi_1(t)dt = A\sqrt{\frac{2}{T_s}}, \quad x_{c1,\phi_2} = \int_{T_s}^{\infty} x_{c1}(t)\phi_2(t)dt = 0. \tag{2.21}$$

Similarly, the projection of x_{c2} along the two axes in the constellation diagram is given by

$$x_{c2,\phi_1} = \int_{T_s}^{\infty} x_{c2}(t)\phi_1(t)dt = -A\sqrt{\frac{2}{T_s}}, \quad x_{c2,\phi_2} = \int_{T_s}^{\infty} x_{c2}(t)\phi_2(t)dt = 0. \tag{2.22}$$

Here, x_{c1} and x_{c2} are two points on the plane of basis functions. Both constellation points lie along the $\phi_1(I)$ axis with no component along $\phi_2(Q)$. Furthermore, the two constellation points are $\theta = \pi$ degrees from each other.

Therefore, each point in a signal constellation diagram has an associated transmitted energy. Thus, for BPSK signals, the energy for first constellation as

$$E_{x_{c1}} = \sqrt{x_{c1,\phi_1}^2 + x_{c1,\phi_2}^2} = \frac{A^2 T_s}{2}, \tag{2.23}$$

Finally, the transmitted energy per bit is given by averaging the energy per bit corresponding to each signal point in the constellation as

$$E_b = \frac{A^2 T_s}{2}. \tag{2.24}$$

The bit error probability for x_{c1} is given by

$$\begin{aligned} p_e &= \frac{1}{2}\left[\int_{-\infty}^{0} \frac{1}{\sqrt{\pi N_0}} e^{\frac{-(r-\sqrt{E_b})}{N_0}} dr + \int_{0}^{\infty} \frac{1}{\sqrt{\pi N_0}} e^{\frac{-(r+\sqrt{E_b})}{N_0}} dr\right] \\ &= \frac{1}{2\sqrt{\pi}}\left[\int_{-\infty}^{-\sqrt{\frac{E_b}{\pi N_0}}} e^{-z^2} dz + \int_{\sqrt{\frac{E_b}{\pi N_0}}}^{\infty} e^{-z^2} dz\right] \\ &= \frac{1}{\sqrt{\pi}} \int_{\sqrt{\frac{E_b}{N_0}}}^{\infty} e^{-z^2} dz \\ &= \frac{1}{2} erfc\left(\frac{E_b}{N_0}\right), \end{aligned} \tag{2.25}$$

where

$$erfc(z) = \frac{2}{\sqrt{\pi}} \int_{\sqrt{z}}^{\infty} e^{-z^2} dz \tag{2.26}$$

is the complementary error function. If the probability of x_{c1} is the same as the probability of x_{c2} i.e. $p(e|x_{c1}) = p(e|x_{c2}) = 1/2$, then the total bit error probability for AWGN channel is written as

$$p_{e,bpsk} = \frac{1}{2} erfc\left(\frac{E_b}{N_0}\right) = Q\left(\sqrt{\frac{E_b}{N_0}}\right). \tag{2.27}$$

Similarly, the instantaneous E_b/N_o over a Rayleigh fading channel β can be expressed as

$$\gamma = \beta E_b / N_0. \tag{2.28}$$

If β is Rayleigh distributed, then the channel β is a Rayleigh fading channel, and the PFD of γ is given by

$$p(\gamma) = \frac{1}{\overline{\gamma}} exp(-\frac{\gamma}{\overline{\gamma}}), \tag{2.29}$$

where the average $\overline{\gamma} = E(\beta^2) E_b/N_o$. Therefore, the BER over β channel can be given as

$$p(\gamma) = \int p_e(\gamma) p(\gamma) d\gamma. \tag{2.30}$$

Thus, the BER of BPSK over β is given as

$$\begin{aligned} p_{bpsk} &= \int_0^\infty p_e(\gamma)p(\gamma)d(\gamma) \\ &= \int_0^\infty Q\left(\sqrt{2\gamma}\right)p(\gamma)d(\gamma) \\ &= \int_0^\infty Q\left(\sqrt{2\gamma}\right)\frac{1}{\overline{\gamma}}exp(-\frac{\gamma}{\overline{\gamma}})d(\gamma) \\ &= \frac{1}{2}(1-\sqrt{\frac{\overline{\gamma}}{\overline{\gamma}}+1}). \end{aligned} \tag{2.31}$$

On the other hand, quadrature phase shift keying (QPSK) is one example of M-ary PSK modulation scheme where it simultaneously transmits 2 bits per symbol. The phase carrier takes one of four equally spaced values (constellation points), such as $\pi/4$, $3\pi/4$, $5\pi/4$ and $7\pi/4$ with $\theta = \pi/2$, where each value of phase corresponds to a unique pair of information bits taking $00, 01, 11, 10$ as shown in Figure 2.10.

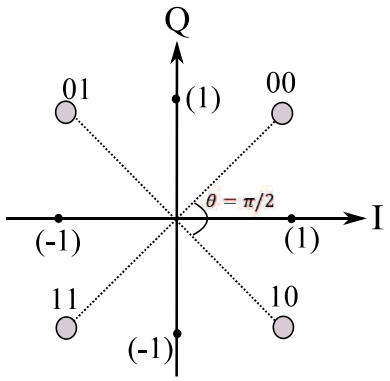

Figure 2.10: Constellation diagram of a QPSK

As usual, for every symbol period, one from the four symbols for transmission during the same symbol period is selected. However in this case, each symbol represents two information bits and therefore the symbol period is twice the bit period. Thus, the expression for the signal x_{c1} that corresponds to the first constellation point is

$$\begin{aligned} x_{c1}(t) &= \frac{A}{\sqrt{2}}cos2\pi f_c t - \frac{A}{\sqrt{2}}sin2\pi f_c t, \\ &= \frac{A}{2}\sqrt{T_s}\phi_1(t) + \frac{A}{2}\sqrt{T_s}\phi_2(t). \end{aligned} \tag{2.32}$$

Then the projection of x_{c1} on the axes representing the two basis functions are

$$x_{c1,\phi_1} = \int_T^{\infty} x_{c1}(t)x_{c1}(t)dt = \frac{A^2T_s}{2}. \tag{2.33}$$

For QPSK, one symbol represents two data bits, which means that the energy per bit is one-half the energy per symbol. The corresponding energy for the first constellation point is given by

$$E_{x_{c1}} = \int_T^{\infty} x_{c1}(t)x_{c1}(t)dt = \frac{A^2T_s}{2}. \tag{2.34}$$

By symmetry, the energy of other constellation points within one symbol period is $(A^2T_s)/2$, and thus the transmitted energy per symbol is $(A^2T_s)/2$. Finally, the transmitted energy per bit is given by averaging the energy per bit corresponding to each signal point in the constellation is written as

$$E_b = \frac{1}{2}\frac{A^2T}{2} = \frac{A^2T_s}{4}. \tag{2.35}$$

Analysis shows that this may be used either to double the data rate compared to a BPSK system while maintaining the bandwidth of the signal or to maintain the data-rate of BPSK but halve the bandwidth needed.

The bit error probability of QPSK is the same as BPSK, and can be written as

$$p_{b,qpsk} = \frac{1}{2}erfc\left(\frac{E_b}{N_0}\right). \tag{2.36}$$

At the same time. the BER of QPSK is the same with BPSK of Eq.(2.31), and be expressed as

$$p_{qpsk} = \frac{1}{2}(1 - \sqrt{\frac{\overline{\gamma}}{\overline{\gamma}+1}}). \tag{2.37}$$

Note that special characteristics of QPSK are twice data can be sent in the same bandwidth compared to BPSK and QPSK has identical bit error probability to that of BPSK. When QPSK is compared to that of BPSK, QPSK provides twice the spectral efficiency with the same energy efficient.

2.3.2 16QAM

Quadirature amplitude phase (QAM) is a modulation technique where its amplitude is allowed to vary with phase [17]. QAM modulation can be viewed as a combination

of amplitude shift keying (ASK) as well as PSK. Also, it can be viewed as ASK in two dimension. The advantage of using QAM is that it is a higher order form of modulation and as a result it is able to carry more bits of information per symbol. By selecting a higher order format of QAM, the data rate of a link can be increased.

Figure 2.11 shows the constellation diagram of 16-ary QAM (16QAM) where it simultaneously transmits 4 bits per symbol. The constellation consists of a square lattice of signal points.

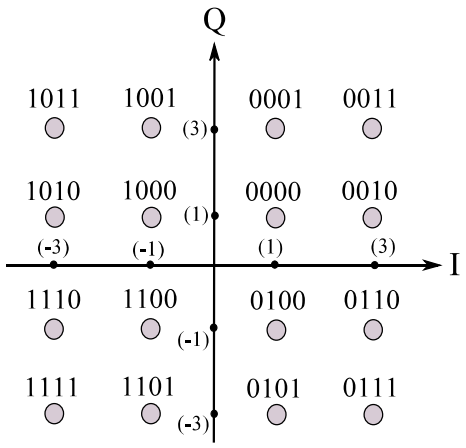

Figure 2.11: Constellation diagram of a 16QAM system

The amplitudes of 16QAM are 3, 1, -1, -3, and its corresponding constellation points are given in Table 2.1.

Table 2.1: Amplitudes and constellations of 16QAM

data bits	Amplitude of I axis	data bits	Amplitude of Q axis
00	-3	00	-3
01	-1	01	-1
10	1	10	1
11	3	11	3

The bit error probability of 16QAM is given by

$$p_{b,16qam} = \frac{3}{8} erfc\left(\frac{4E_b}{10N_0}\right). \tag{2.38}$$

Theoretically, 16QAM enables data to be transmitted in a much smaller spectrum. However, the symbols are easily subjected to errors due to noise and interference because the symbols are located very closed together in the constellation diagram. Thus such signal has to transmit extra power so that the symbol can be spread out more and this reduces power efficiency as compared to BPSK and QPSK modulation. The computer simulation will be given to clarify the BER of these modulation schemes in AWGN and Rayleigh fading channel, respectively.

Figure 2.12 shows the BER performance of the BPSK, QPSK and 16QAM modulation schemes for AWGN channel with the total number of transmitting data bits are 10000. In this simulation, the BER is obtained by varying the values of E_b/N_0 in the range of 0 to 14 dB. It is observed that the BER performance of BPSK is close to the theoretical result. Similarly, in the case of E_b/N_0, the BER performance of BPSK and QPSK is same in the same transmission rate. The BER performance of 16QAM is decreases about 4 dB for 10^{-4} that of BPSK and QPSK. Furthermore, the simulation and theoretical results of these modulation schemes are almost same.

Similarly, Figure 2.13 shows the BER performance of the BPSK, QPSK and 16QAM modulation schemes for fading channel with the total number of transmitting data bits are 10000. It is shown that the BER of BPSK and QPSK is same in the same transmission rate. The BER performance of 16QAM is decreases about 4 dB for 10^{-2} that of BPSK and QPSK. Furthermore, the simulation and theoretical results of these modulation schemes are almost same.

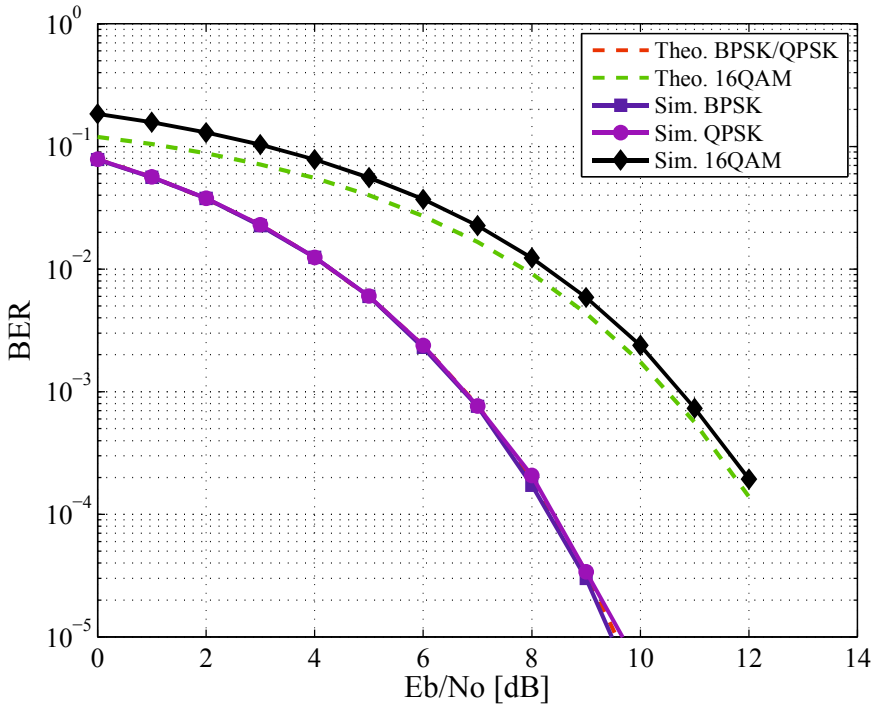

Figure 2.12: BER performance of modulation schemes in AWGN channel

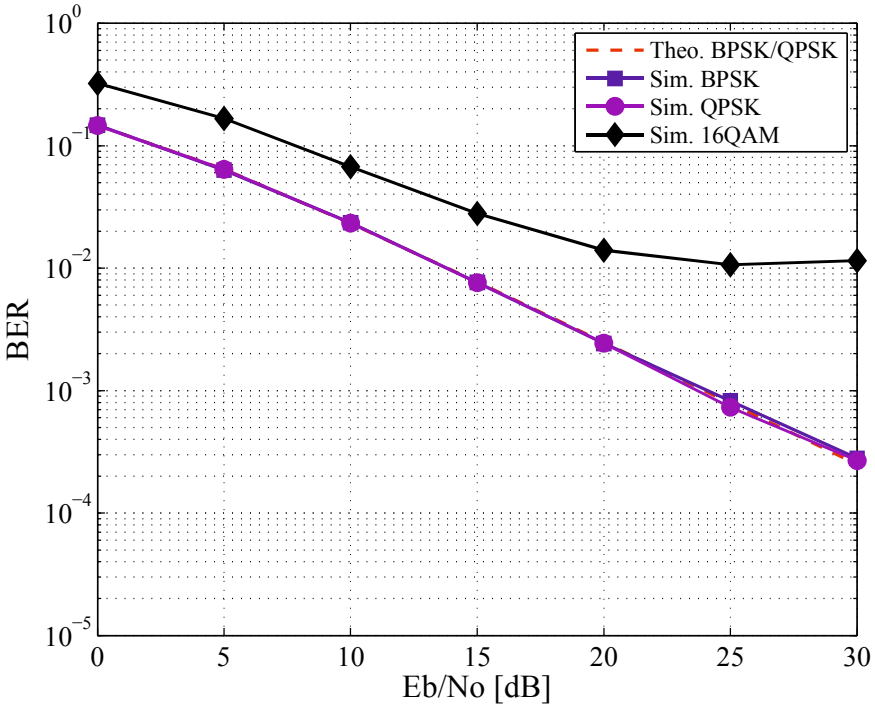

Figure 2.13: BER performance of modulation schemes in Rayleigh fading channel

2.4 Singlecarrier and Multicarrier Schemes

In this section, direct sequence code division multiple access (DS-CDMA), orthogonal frequency division multiplexing (OFDM) and multicarrier code division multiple access (MC-CDMA) including multicarrie direct sequence code division multiple access (MC-DS-CDMA) are introduced and reviewed.

2.4.1 DS-CDMA

One of the basic concepts in data communication is the idea of allowing several transmitters to send data bits over a single communication channel [1], [2] . This allows several users to share a band of frequencies. This concept called multiple access. CDMA employs spread spectrum technology and a special coding scheme where each transmitter is assigned a sequence in a set of sequences (code) to allow multiple users to be multiplexed over the same physical channel [3]. There are two kinds of transmissions such as synchronous and asynchronous CDMA transmission as shown in Figure 2.14. The former is applied when there is a need to maintain accurate synchronicity among all multiple users. At the same time, the latter allows to several delays among all multiple users [13], [14].

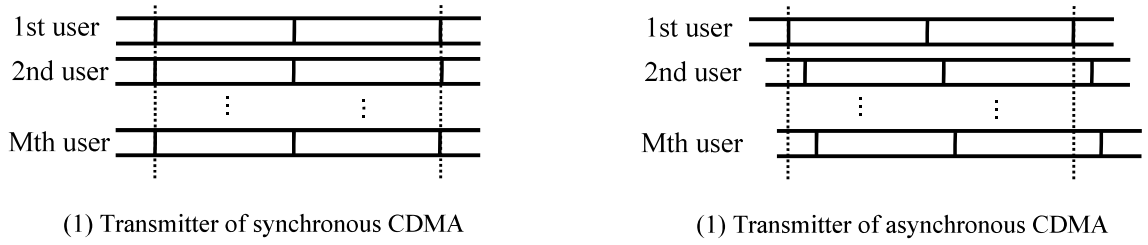

Figure 2.14: Synchronous and asynchronous CDMA

DS-CDMA is one of the singlecarrier scheme, and it spreads the original data symbols using a given spreading sequence in the time domain [7] [11]. The capability of reducing the inter symbol interference (ISI) due to multipath and multiple access interference (MAI) induced by adjacent multiple users are determined by the correlation properties of the spreading sequences. Figure 2.15(a) illustrates a basic model of DS-CDMA for a single user m.

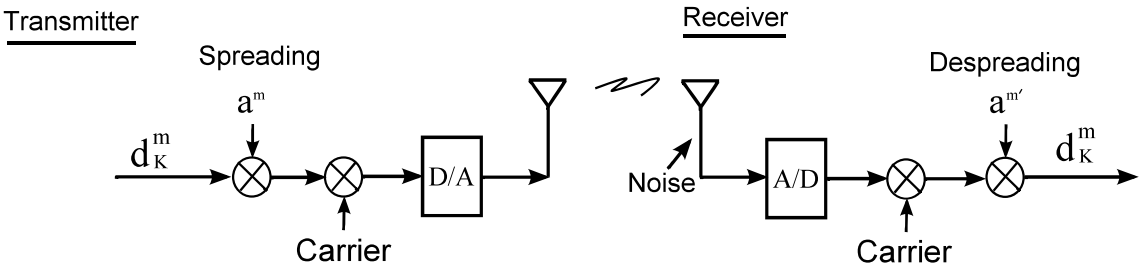

(a) The transmitter and receiver of DS-CDMA

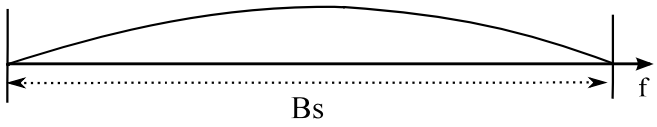

(b) Spectrum of DS-DMA transmitted signal

Figure 2.15: A basic model of DS-CDMA and its frequency spectrum

At the transmitter, the modulated data symbols d_k with binary data bits $k = (1 - 111 - 1)$ (here, BPSK modulation is assumed) of user m is first multiplied by a spreading sequence $a^m = (a_0^m, a_1^m, \cdots . a_n^m, \cdots, a_{N-1}^m)$ of length N. This causes the spectrum of the information signal to be spread across the allocated bandwidth as shown in Figure 2.15(b). Next, the spread signal is modulated onto its carrier before it is transmitted as given in Figure 2.16. The transmitted signal is given by

$$s^m(t) = Ad_k^m(t)a^m(t)e^{j2\pi f_c t}, \tag{2.39}$$

where A is the amplitude and f_c is the central frequency of the carrier signal.

At the receiver, the transmitted signal of mth user passed through multipath propagation channel and plus AWGN is received. The received signal is given by

$$r^m(t) = s^m(t - \tau_j) + n(t), \tag{2.40}$$

where τ_j is the propagation delay from the transmitter to the receiver of the jth path for user m and n is the AWGN. Let us now concentrate on the recovery of the transmitting data symbols.

The received signal can be rewritten as

$$r^m(t) = s^m(t - \tau_j),$$

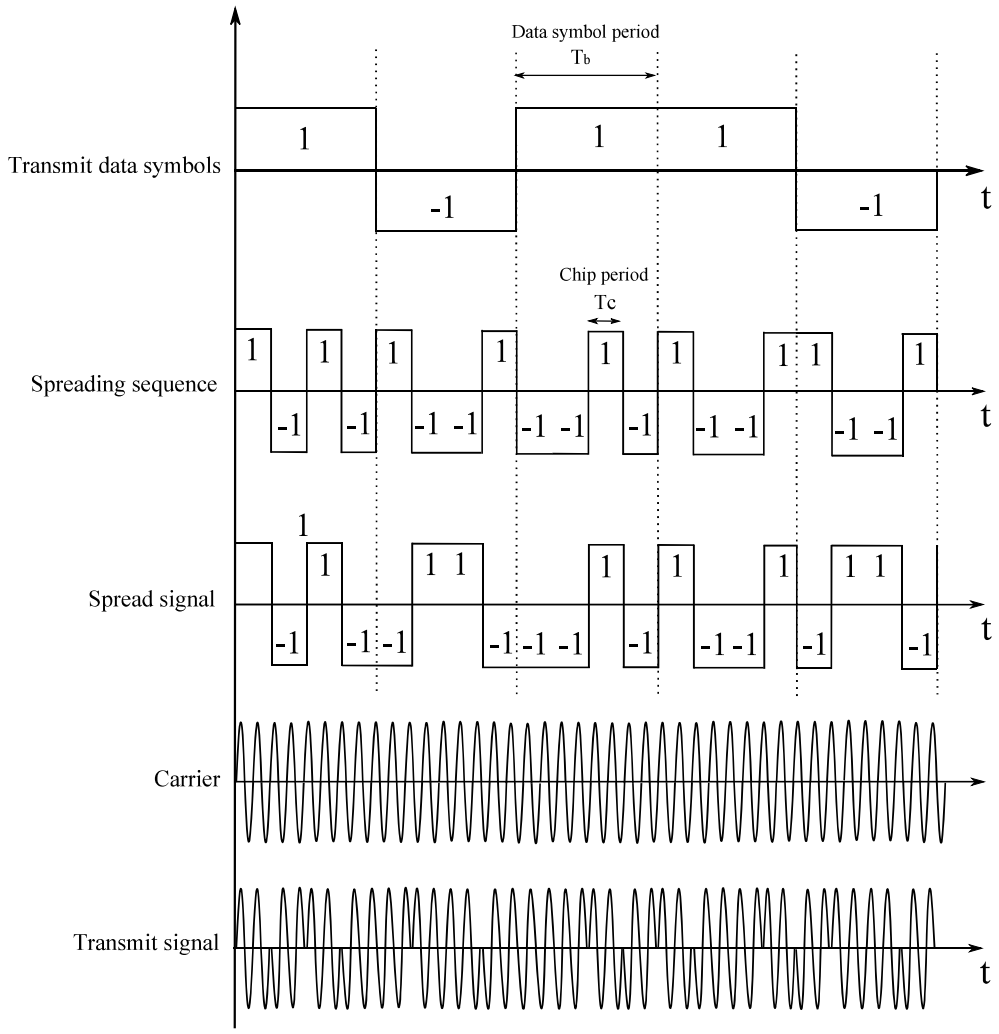

Figure 2.16: Spectrum spreading in DS-CDMA for transmitter

$$= Ad_k^m(t-\tau_j)a^m(t-\tau_j)e^{j2\pi f_c t+\theta}, \tag{2.41}$$

where the propagation delay induced carrier shift is given by $\theta = -2\pi f_c \tau_j$. For simplicity, a synchronous system with $\theta = 0$ is assumed.

In order to recover the original data symbols of user m, the received signal is despread by multiplying the received signal with a synchronized replica of the spreading sequence $a^{m'}$ of user m, as follows

$$\begin{aligned}\hat{s}^m(t) &= r^m(t)a^{m'}(t-\tau_j'), \\ &= Ad_k^m(t-\tau_j)a^m(t-\tau_j)a^{m'}(t-\tau_j')e^{j2\pi f_c t}, \end{aligned} \tag{2.42}$$

where τ_j' is the delay estimate.

In order to demodulate the signal, it is then multiplied by the carrier and passed through a correlator, then we have

$$z^m = \int_t^{t+T_b} \hat{s}(t) e^{-j2\pi f \tau} dt. \tag{2.43}$$

If it is assumed that the replica of the spreading code at the receiver is orthogonal to the sequence used to spread the signal at the transmitter, then $\tau_j = \tau_j'$ and we can set $\tau_j = 0$, by Eq. 2.43, can be written as

$$\hat{s}^m(t) = A d_k^m(t) a^2(t) e^{j2\pi f_c t}. \tag{2.44}$$

The high frequency term $e^{j2\pi f_c t}$ tends to zero after the correlator-based receiver. By Eqs.2.43 and 2.44, the resulting in an equal number of positive and negative terms in the integral, yielding

$$z^m = \int_t^{t+T_b} A d_k^m(t) a^2(t) dt. \tag{2.45}$$

Since it is assumed that there is no timing error, $d^m(t)$ is BPSK demodulated, giving $d^m(t) = \pm 1$, and $\int_0^{T_b} a^2(t) = T_b$, hence we have

$$z^m = \pm \frac{A T_b}{2}. \tag{2.46}$$

Note that the spreading sequences have to be carefully designed in order to have low correlation values, and an issue to be addressed in chapter 3 in depth.

2.4.2 OFDM

The increasing require for high data rate wireless communications has incited the appearance of OFDM for achieving good performance [57]- [59]. It is also an effective technique that provides a high spectral efficiency and to combat multipath frequency selective fading fading channels without losing orthogonality of the neighboring subcarriers. However, OFDM has some weakness such as difficulty in subcarrier synchronization, sensitivity to frequency offset and nonlinear amplification. The basic model of an OFDM is illustrated in Figure 2.17.

At the transmitter, the modulated data symbols $d^m = (d_0^m, d_1^m, \cdots, d_k^m, \cdots, d_{K-1}^m) \in C$ of mth user are serial-to-parallel (S/P) converted into d_k^m data sequences and allocated over different orthogonal subcarriers using N-point inverse discrete Fourier

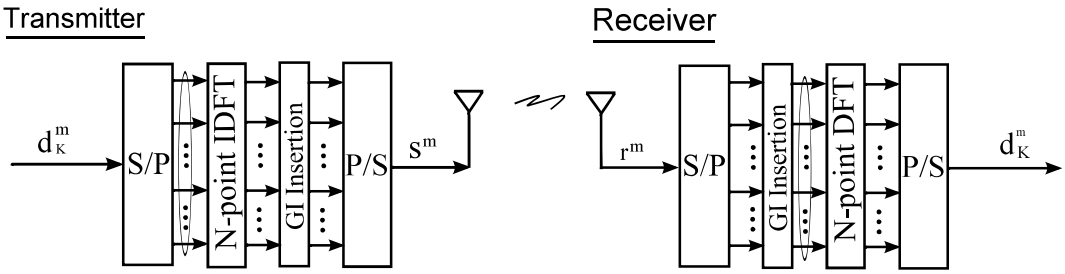

Figure 2.17: A basic model of OFDM

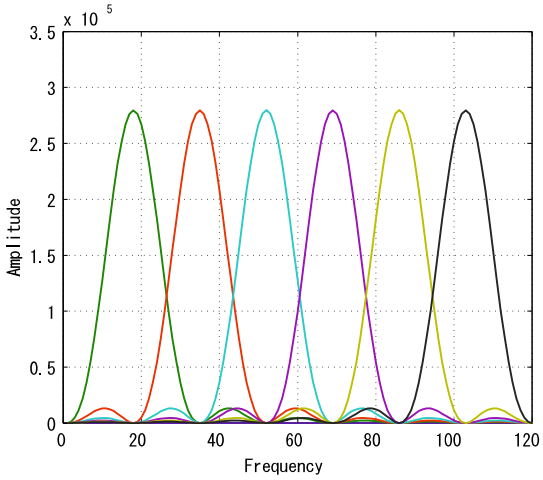

Figure 2.18: OFDM subcarriers spectrum

transform (IDFT) as shown in Figure 2.18 . A guard interval (GI) is inserted in each OFDM symbol to prevent inter symbol interference (ISI) and inter carrier interference (ICI) due to multipath as shown in Figure 2.7. The signal is transmitted after parallel-to-serial (P/S) conversion.

The transmitted signal of the mth user can be expressed as

$$s^m(t) = \sum_{i=0}^{N_d-1} g(t-iT).\{\sqrt{\frac{2P}{N_c}} \sum_{n=0}^{N_c-1} d_{n,i}^m e^{\frac{j2\pi(t-iT)n}{T_s}}\}, \tag{2.47}$$

where $N_d = K$ and N_c are the number of data symbols and number of subcarriers. T_s is effective symbol length and P is the average transmission power per user. Moreover, symbol length $T = T_g + T_s$, where T_g is the GI length. $g(t)$ is the

transmission pulse given by

$$g(t) = \begin{cases} 1 & \text{for } -T_g \leq t \leq T_s, \\ 0 & \text{otherwise.} \end{cases} \tag{2.48}$$

At the receiver, the received signal passed multipath fading channel of Eq.(2.10) can be expressed as

$$r^m(t) = \int_0^\infty p^m(\tau, t) s^m(t-\tau) d\tau + \eta^m(t), \tag{2.49}$$

where $\eta^m(t)$ is the AWGN with a signal sided power spectral density of N_0. After S/P conversion and GI removal, the frequency domain signal of Eq.(2.49) is given by

$$\begin{aligned} r^m_{n,i} &= \sum_{n=0}^{N_c-1} r^m(t) e^{\frac{-j2\pi(t-iT)n}{T_s}} \\ &= \sqrt{\frac{2P}{N_c}} H^m_{n,i} u^m_{n,i} + \eta^m_{n,i}. \end{aligned} \tag{2.50}$$

where $u^m_{n,i}$ is outputs of N-point DFT, $H^m_{n,i}$ is the channel transfer function and $\eta^m_{n,i}$ is AWGN noise with zero-mean and a variance of $2N_0/T_s$. Finally, the original data symbols d^m_K is recovered by demodulation.

2.4.3 MC-CDMA

This subsection introduce the class of multicarrier CDMA schemes [5]. Specifically, review their design parameters, spectral characteristics, advantages and disadvantages in terms of the transmitter and receiver structures as well as their spectral efficiency.

In recent years, multicarrier CDMA schemes including MC-CDMA using frequency domain spreading and MC-DS-CDMA using time domain spreading based on the combination of OFDM and CDMA has been receiving widespread interests for wireless communications [6], [61]. These schemes benefit from the main advantages of both techniques such as high spectral efficiency, robustness to frequency selective fading channels, multiple access capability and high frequency diversity achievement. In two schemes, the orthogonality of neighboring subcarriers is satisfied with minimum frequency separation as shown in Figures 2.20 and 2.22, respectively.

Figure 2.19 illustrates the basic model of MC-CDMA for a single user m.

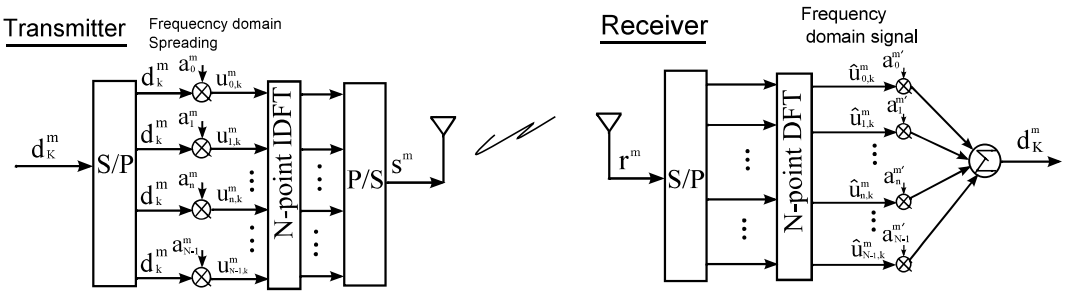

Figure 2.19: The concept of a MC-CDMA

At the MC-CDMA transmitter, the modulated data symbols d_K^m after S/P conversion is first multiplied with the spreading sequence a^m of length N of the mth user in frequency domain, and then modulated into different subcarriers signals using the N-point IDFT. Its frequency spectrum is shown in Figure 2.20. Finally, MC-CDMA signal s^m is transmitted after P/S conversion. In general, the length of subcarries is equal to N.

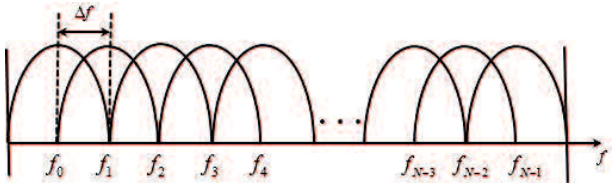

Figure 2.20: The spectrum of the MC-CDMA signal

At the receiver, after P/S conversion, the received signal is converted into frequency domain signal with different frequencies by applying N-point DFT. Finally, the original data symbol d_K^m is detected by de-spreading (or inner product) of the spreading sequence $a^{m'}$ and the frequency domain sequence $\hat{u}^m$.

On the other hand, Figure 2.21 illustrates the basic model of MC-DS-CDMA for a single user m. At the transmitter, the modulated data symbols d_K^m after S/P conversion is first multiplied with the spreading sequence a^m of length N of the mth user in time domain, and then modulated into different subcarriers signals using the N-point IDFT. Its frequency spectrum is shown in Figure 2.22. Finally, MC-DS-CDMA signal s^m is transmitted after P/S conversion. In general, the length of

subcarries is equal to the length of data symbols K.

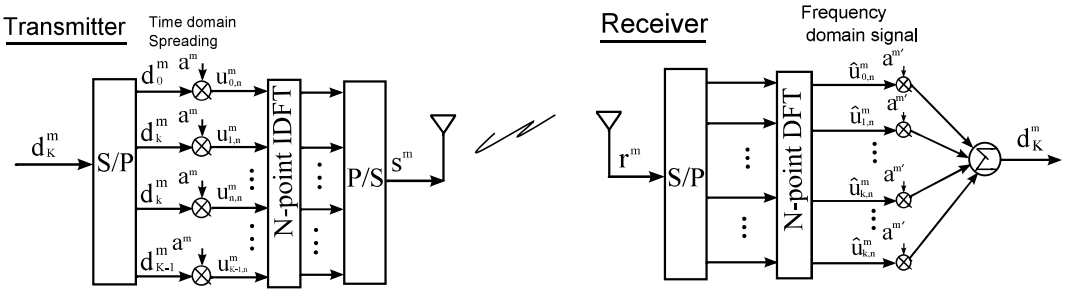

Figure 2.21: The concept of a MC-DS-CDMA

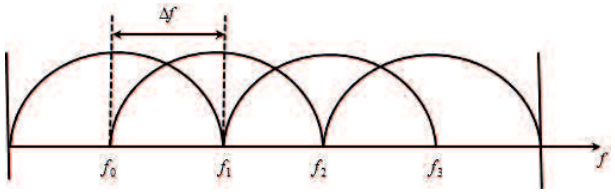

Figure 2.22: The spectrum of the MC-DS-CDMA signal

At the receiver, after P/S conversion, the received signal is converted in to frequency domain signal with different frequencies by applying N-point DFT. Finally, the original data symbol d_K is detected by de-spreading (or inner product) of the spreading sequence $a^{m'}$ and the frequency domain sequence $\hat{u}^m$.

It is known that MC-CDMA possess better system performance than MC-DS-CDMA [5], [6], [42], since the former provides higher frequency diversity. So, this dissertation discusses on MC-CDMA using some effective sets of spreading sequences such as zero correlation zone (ZCZ) code and some novel interference cancellation methods to mitigate the ISI and ICI due to multipath, and MAI from adjacent users. Their detail will be presented in the next chapters in depth.

Chapter3

ZCZ Code and ZCZ-CDMA Schemes

In this chapter, firstly, the introduction of zero correlation zone (ZCZ) code with low correlation properties is given and its orthogonality for time domain and frequency domain on the Fourier transforms is clarified. Next, DS-CDMA using ZCZ code is presented. Furthermore, MAI-free BC-DS-ZCZ-CDMA scheme is introduced and its problem is depicted. Finally, MC-CDMA using ZCZ code without GI technique is introduced and its problem is also depicted.

3.1 ZCZ Code

In this section, four kinds of sets of orthogonal sequences (codes) of length $N = 2^{\kappa}$ including shift orthogonal codes, i.e., ZCZ code, are introduced and their correlation properties are compared [51]- [54]. There are a general orthogonal (GO) code whose code words are corresponding to rows in the Sylvester type Hadamard matrix, a code by GO code and E-sequences called EO code, whose aperiodic autocorrelation function takes zero at even shifts except zero-shift, codes produced by GO code and EO code called GZCZ code and EZCZ code, respectively.

3.1.1 Introduction of ZCZ Code

Let us consider an orthogonal code of length $N = 2^\kappa$ defined by

$$\left.\begin{aligned} A &= \{\mathbf{a}^0, \mathbf{a}^1, \cdots, \mathbf{a}^m, \cdots, \mathbf{a}^{M-1}\}, \\ \mathbf{a}^m &= (a_0^m, a_1^m, \cdots, a_n^m, \cdots, a_{N-1}^m). \end{aligned}\right\} \tag{3.1}$$

Concentrate on a Hadamard matrix H_κ of order 2^κ defined by $H_\kappa H_\kappa^T = H_\kappa^T H = 2^\kappa I$, where I denotes the unit matrix of order 2^κ and T the transpose of the matrix.

Let H_κ be the Sylvester type Hadamard matrix defined by

$$H_\kappa = \left(h_{m,n} \right)_{0 \le m,n < 2^\kappa}, \quad H_1 = \begin{pmatrix} 1 & 1 \\ 1 & -1 \end{pmatrix}. \tag{3.2}$$

GO code of of length $N = 2^\kappa$ defined by a set of rows of H_κ is expressed by

$$A_{GO} = H_\kappa. \tag{3.3}$$

The aperiodic correlation function between two bi-phase sequence a^m and $a^{m'}$ with length N at a shift τ is defined by

$$C_{a^m a^{m'}}(\tau) = \begin{cases} \sum_{n=0}^{N-1-\tau} a_n^m a_{(n+\tau)}^{m'} & 0 \le \tau \le N-1, \\ \sum_{n=0}^{N-1+\tau} a_{(n-\tau)}^m a_n^{m'} & 1-N \le \tau < 0, \\ 0 & |\tau| \ge N. \end{cases} \tag{3.4}$$

Similarly, the periodic correlation function is defined by

$$\begin{aligned} R_{a^m a^{m'}}(\tau) &= \sum_{n=0}^{N-1} a_n^m a_{(n+\tau) \bmod N}^{m'} \\ &= C_{a^m a^{m'}}(\tau) + C_{a^m a^{m'}}(\tau - N). \end{aligned} \tag{3.5}$$

If the aperiodic auto-correlation function of the bi-phase sequence a^m is zero at any even shift $\tau \neq 0$ can be written as

$$C_{a^m a^{m'}}(2\tau) = \begin{cases} N & (\tau = 0), \\ 0 & (\tau \neq 0). \end{cases} \tag{3.6}$$

Then, a set of A is called even-shift orthogonal codes (E-codes) [53]. Therefore, the periodic auto-correlation function takes zero at any even-shift can be written as

$$R_{a^m a^{m'}}(\tau) = C_{a^m a^{m'}}(\tau) + C_{a^m a^{m'}}(\tau - N) = \begin{cases} N & (\tau = 0), \\ 0 & (\tau \neq 0). \end{cases} \tag{3.7}$$

For example, $a^m = (1, 1, 1, 1, 1, -1, -1, 1)$ is an E-sequence of length $N = 8$, and its aperiodic auto-correlation function is shown in Figure 3.1. It is shown that the E-code's aperiodic auto-correlation function takes high pick value at shift $\tau = 0$, and the sidelobes are constrained with zero at any even shift, respectively.

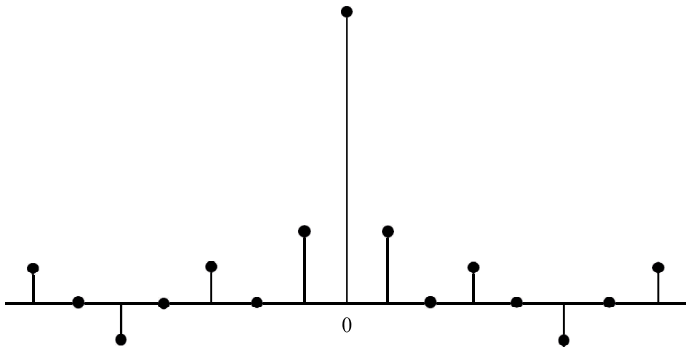

Figure 3.1: Aperiodic auto-correlation function of E-code

It is known that E-code is included in complementary sequences [50]. EO code is defined by

$$A_{EO} = H_\kappa \delta_k, \tag{3.8}$$

where δ_κ is a diagonal matrix of order 2^κ whose diagonal elements equal complementary sequences which including E-sequence e expressed by.

$$\delta_\kappa = \begin{pmatrix} g_{00} & \cdots & 0 & \cdots & 0 \\ 0 & \ddots & 0 & \cdots & 0 \\ \vdots & \cdots & g_{xx} & \cdots & 0 \\ 0 & \cdots & 0 & \ddots & 0 \\ 0 & \cdots & 0 & \cdots & g_{(\kappa-1)(\kappa-1)} \end{pmatrix}, \tag{3.9}$$

where $g_{xx} = (-1)^{g(\vec{x})}$ is a different expressions which will be introduced in next subsection. So that ZCZ codes with good correlation properties can be constructed by selecting δ_κ properly.

ZCZ code denoted by $Z(N, M, Zcz)$ is a set of M sequences of length N with a zero correlation zone (Zcz), if the periodic correlation function between sequences a^m and $a^{m'}$ defined by

$$R_{a^m a^{m'}}(\tau) = \sum_{n=0}^{N-1} a_n^m a_{(n+\tau) mod N}^{m'} \tag{3.10}$$

is written as

$$R_{a^m a^{m'}}(\tau) = \begin{cases} N & \text{for } \tau = 0, m = m', \\ 0 & \text{for } \tau = 0, m \neq m', \\ 0 & \text{for } 1 \leq \mid \tau \mid \leq Zcz. \end{cases} \tag{3.11}$$

Figure 3.2 shows the periodic auto and cross-correlation functions of ZCZ code.

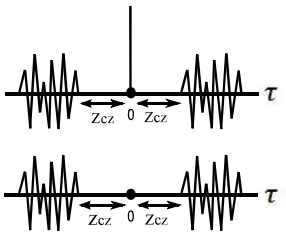

Figure 3.2: Periodic auto and cross-correlation functions of ZCZ code.

Note that if $Zcz = 0$, the set denotes an orthogonal code with $N = M$. ZCZ code [25] is bounded by

$$M \leq \frac{N}{Zcz + 1}. \tag{3.12}$$

ZCZ code with $Zcz = 1$ is discussed, because of achieving the upper bound of Eq.(3.12).

GZCZ code $Z(2^\kappa, 2^{\kappa-1}, 1)$ is defined by

$$A_{GZCZ} = \begin{bmatrix} a^0 \\ a^1 \\ \vdots \\ a^m \\ \vdots \\ a^{2^{\kappa-1}} \end{bmatrix} = [H_{\kappa-1}, H_{\kappa-1}\zeta_{\kappa-1}], \tag{3.13}$$

where $\zeta_{\kappa-1}$ is a diagonal matrix of order $2^{\kappa-1}$ defined by $\zeta_{\kappa-1} = diag(-1, 1, -1, 1, \cdots, -1, 1)$.

Similarly, EZCZ code $Z(2^\kappa, 2^{\kappa-1}, 1)$ is defined by

$$A_{EZCZ} = \begin{bmatrix} a^0 \\ a^1 \\ \vdots \\ a^m \\ \vdots \\ a^{2^{\kappa-1}} \end{bmatrix} = [H_{\kappa-1}\delta_{\kappa-1}, H_{\kappa-1}\delta_{\kappa-1}\zeta_{\kappa-1}]. \tag{3.14}$$

Figures 3.3 and 3.4 show the periodic auto and cross-correlation functions of the four types of orthogonal codes with length $N = 32$, respectively. It is observed that the EZCZ code has the best auto and cross-correlation properties with low sidelobes, and it could be utilize for CDMA schemes in high data rate transmissions with large delay spread.

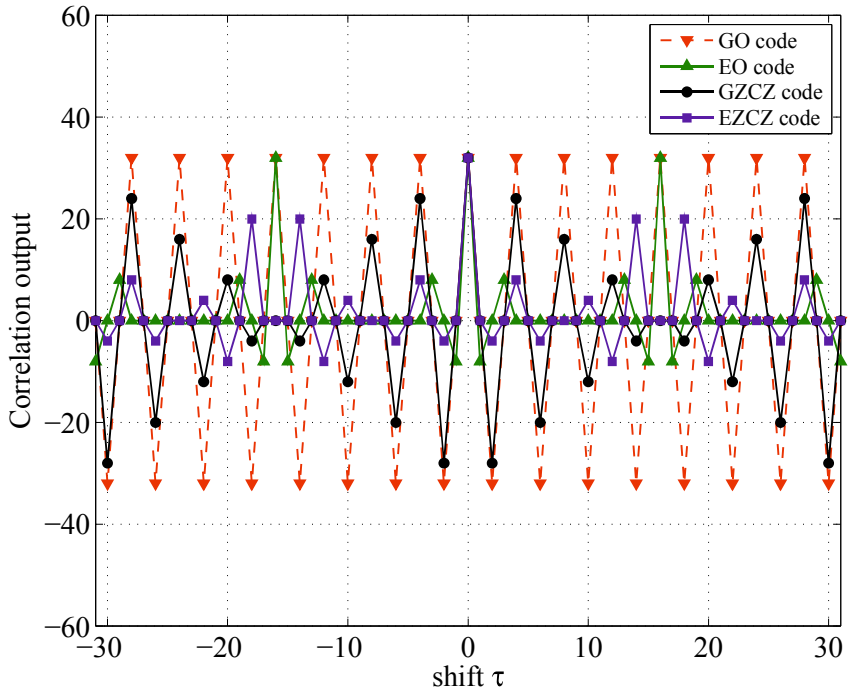

Figure 3.3: Periodic auto-correlation function of orthogonal codes with length $N = 32$

The logic functions of the orthogonal codes introduced in the above subsection are investigated. Let $\vec{x} = (x_0, x_1, \ldots, x_{\kappa-1})$ be the space V_κ of binary κ-tuples, whose elements are coefficients expressed as the binary expansion of an integer $x(0 \leq x < 2^\kappa - 1)$, i.e.,

$$x = x_0 2^0 + x_1 2^1 + \ldots + x_{\kappa-1} 2^{\kappa-1}. \tag{3.15}$$

Let us consider the logic functions of an orthogonal code A of length 2^κ, which is expressed by

$$a_x^m = (-1)^{f_A(m,x)}. \tag{3.16}$$

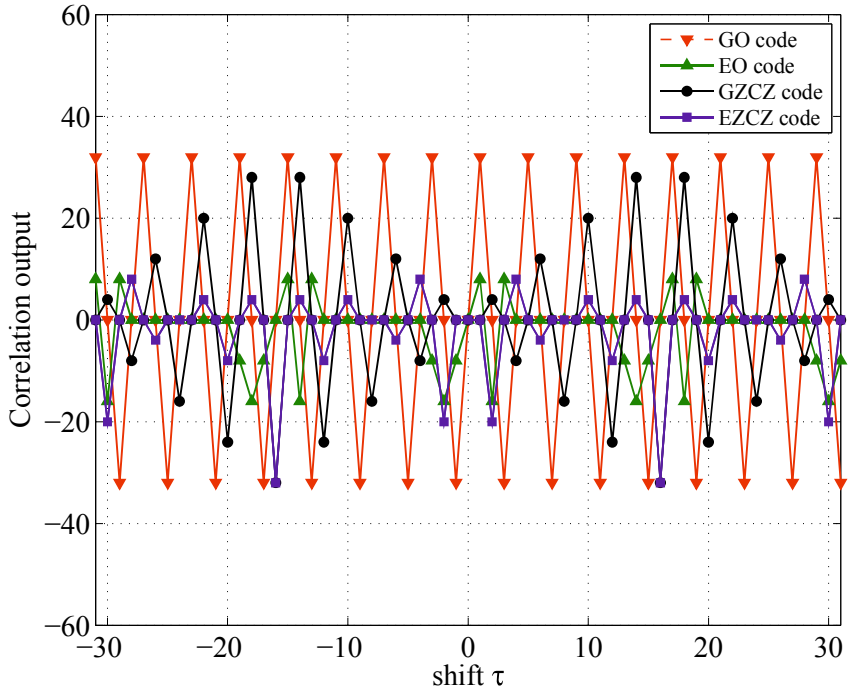

Figure 3.4: Periodic cross-correlation function of orthogonal codes with length $N = 32$

The logic functions of the orthogonal codes A_{GO} and A_{EO} of length 2^κ are respectively given by

$$f_{A_{GO}}(m, x) = m_0x_0 \oplus m_1x_1 \oplus \cdots \oplus m_{\kappa-1}x_{\kappa-1}, \tag{3.17}$$

$$f_{A_{EO}}(m, x) = m_0x_0 \oplus m_1x_1 \oplus \cdots \oplus m_{\kappa-1}x_{\kappa-1} \oplus y_0y_1 \oplus y_1y_2 \oplus \ldots \oplus y_{\kappa-2}y_{\kappa-1} \tag{3.18}$$

where $\oplus$ denotes the addition over2, i.e., EXOR, and $y_j \in \{x_0, x_1, \cdots, x_{\kappa-1}\}$ with $y_0 = x_0$ or $y_{\kappa-1} = x_0$ and $y_j \neq y_\kappa$ for $j \neq \kappa(\geq 1)$.

The logic functions show that EO code consists of all E-sequences with good autocorrelation property [52], and the logic function with $y_0 \neq x_0$ or $y_{\kappa-1} \neq x_0$ generates ZCZ code consisting of complementary sequences except E-sequences.

Similarly, the logic functions of $Z(2^\kappa, 2^{\kappa-1}, 1)$, A_{GZCZ} and A_{EZCZ}, are respectively given by

$$f_{A_{GZCZ}}(\hat{m}, x) = m_0x_0 \oplus m_1x_1 \oplus \cdots \oplus m_{\kappa-2}x_{\kappa-2} \oplus x_0x_{\kappa-1} \oplus x_{\kappa-1}, \tag{3.19}$$

$$f_{A_{EZCZ}}(\hat{m}, x) = m_0x_0 \oplus m_1x_1 \oplus \cdots \oplus m_{\kappa-2}x_{\kappa-2} \oplus y_1y_2 \oplus \cdots \oplus y_{\kappa-3}y_{\kappa-2} \oplus x_0x_{\kappa-1} \oplus x_{\kappa-1}, \tag{3.20}$$

where $0 \leq \hat{m} \leq 2^{\kappa-1}-1$, and $y_j \in \{x_0, x_1, \cdots, x_{\kappa-1}\}$ with $y_0 = x_0$ and $y_j \neq y_\kappa$ for $j \neq \kappa (\geq 1)$.

Note that EZCZ code consists of complementary sequences except E-sequences [51]. It has been shown that A_{EZCZ} possesses good auto and cross-correlation properties in comparison with A_{GZCZ}.

As an example, EZCZ code $A(16, 8, 1)$ is generated by the logic function in Eq.(3.20) as

$$A(\vec{x}) \;=\; x_0 x_1 \oplus x_1 x_2,$$

which is expressed by

$$A = \underbrace{\begin{pmatrix} 1 & 1 & 1 & 1 & 1 & 1 & 1 & 1 \\ 1 & -1 & 1 & -1 & 1 & -1 & 1 & -1 \\ 1 & 1 & -1 & -1 & 1 & 1 & -1 & -1 \\ 1 & -1 & -1 & 1 & 1 & -1 & -1 & 1 \\ 1 & 1 & 1 & 1 & -1 & -1 & -1 & -1 \\ 1 & -1 & 1 & -1 & -1 & 1 & -1 & 1 \\ 1 & 1 & -1 & -1 & -1 & -1 & 1 & 1 \\ 1 & -1 & -1 & 1 & -1 & 1 & 1 & -1 \end{pmatrix}}_{H_3} \underbrace{\begin{pmatrix} 1 & 0 & 0 & 0 & 0 & 0 & 0 & 0 \\ 0 & 1 & 0 & 0 & 0 & 0 & 0 & 0 \\ 0 & 0 & 1 & 0 & 0 & 0 & 0 & 0 \\ 0 & 0 & 0 & -1 & 0 & 0 & 0 & 0 \\ 0 & 0 & 0 & 0 & 1 & 0 & 0 & 0 \\ 0 & 0 & 0 & 0 & 0 & 1 & 0 & 0 \\ 0 & 0 & 0 & 0 & 0 & 0 & -1 & 0 \\ 0 & 0 & 0 & 0 & 0 & 0 & 0 & 1 \end{pmatrix}}_{\delta_3}$$

$$\times \left(\underbrace{\begin{pmatrix} 1 & 0 & 0 & 0 & 0 & 0 & 0 & 0 \\ 0 & 1 & 0 & 0 & 0 & 0 & 0 & 0 \\ 0 & 0 & 1 & 0 & 0 & 0 & 0 & 0 \\ 0 & 0 & 0 & 1 & 0 & 0 & 0 & 0 \\ 0 & 0 & 0 & 0 & 1 & 0 & 0 & 0 \\ 0 & 0 & 0 & 0 & 0 & 1 & 0 & 0 \\ 0 & 0 & 0 & 0 & 0 & 0 & 1 & 0 \\ 0 & 0 & 0 & 0 & 0 & 0 & 0 & 1 \end{pmatrix}}_{I_3}, \underbrace{\begin{pmatrix} -1 & 0 & 0 & 0 & 0 & 0 & 0 & 0 \\ 0 & 1 & 0 & 0 & 0 & 0 & 0 & 0 \\ 0 & 0 & -1 & 0 & 0 & 0 & 0 & 0 \\ 0 & 0 & 0 & 1 & 0 & 0 & 0 & 0 \\ 0 & 0 & 0 & 0 & -1 & 0 & 0 & 0 \\ 0 & 0 & 0 & 0 & 0 & 1 & 0 & 0 \\ 0 & 0 & 0 & 0 & 0 & 0 & -1 & 0 \\ 0 & 0 & 0 & 0 & 0 & 0 & 0 & 1 \end{pmatrix}}_{\zeta_3} \right),$$

$$= \begin{pmatrix} 1 & 1 & 1 & -1 & 1 & 1 & -1 & 1 & -1 & 1 & -1 & -1 & -1 & 1 & 1 & 1 \\ 1 & -1 & 1 & 1 & 1 & -1 & -1 & -1 & -1 & 1 & -1 & 1 & -1 & -1 & 1 & -1 \\ 1 & 1 & -1 & 1 & 1 & 1 & 1 & -1 & -1 & 1 & 1 & 1 & -1 & 1 & -1 & -1 \\ 1 & -1 & -1 & -1 & 1 & -1 & 1 & 1 & -1 & -1 & 1 & -1 & -1 & -1 & -1 & 1 \\ 1 & 1 & 1 & -1 & -1 & -1 & 1 & -1 & -1 & 1 & -1 & -1 & 1 & -1 & -1 & -1 \\ 1 & -1 & 1 & 1 & -1 & 1 & 1 & 1 & -1 & -1 & -1 & 1 & 1 & 1 & -1 & 1 \\ 1 & 1 & -1 & 1 & -1 & -1 & -1 & 1 & -1 & 1 & 1 & 1 & 1 & -1 & 1 & 1 \\ 1 & -1 & -1 & -1 & -1 & 1 & -1 & -1 & -1 & -1 & 1 & -1 & 1 & 1 & 1 & -1 \end{pmatrix}.$$

Where the row of the matrix corresponds to the length of a sequence $N = 16$ and the column of the matrix corresponds to the family size of code $M = 8$.

3.1.2 Orthogonality on the Fourier Transforms

This subsection clarifies the orthogonality of a phase-shifted symbol sequence in ZCZ code for time domain and frequency domain on the Fourier transforms as IDFT and DFT [21].

DFT of a time domain sequence (vector) $\mathbf{s}^m$ of length N is defined by

$$a_n^m = \frac{1}{\sqrt{N}} \sum_{q=0}^{N-1} s_q^m \omega^{-nq}, \tag{3.21}$$

and IDFT of a frequency domain sequence (vector) $\mathbf{a}^m$ can be expressed by

$$s_q^m = \frac{1}{\sqrt{N}} \sum_{n=0}^{N-1} a_n^m \omega^{nq}, \tag{3.22}$$

where $\omega^q = e^{\frac{j2\pi q}{N}}$.

Let $\mathbf{s}^{m,\tau}$ be a τ phase-shifted sequence of length N defined by

$$\mathbf{s}^{m,\tau} = (s_\tau^m, s_{\tau+1}^m, \cdots, s_{n \bmod N}^m, \cdots, s_{\tau-1}^m). \tag{3.23}$$

DFT of $\mathbf{s}^{\mathbf{m},\tau}$ is written as

$$\mathbf{a}^{m,\tau} = (a_0^m, \omega^\tau a_1^m, \cdots, \omega^{\tau n} a_n^m, \cdots, \omega^{\tau(N-1)} a_{N-1}^m), \tag{3.24}$$

since

$$\begin{aligned} \frac{1}{\sqrt{N}} \sum_{q=0}^{N-1} s_{q+\tau}^m \omega^{-nq} &= \frac{1}{\sqrt{N}} \sum_{q=0}^{N-1} s_q^m \omega^{-n(q-\tau)} \\ &= \omega^{n\tau} \frac{1}{\sqrt{N}} \sum_{q=0}^{N-1} s_q^m \omega^{-nq} \\ &= \omega^{n\tau} a_n^m. \end{aligned} \tag{3.25}$$

Let $\mathbf{a}^m$ be a sequence in ZCZ code $A(N, N/2, 1)$ of Eq.(3.13) or Eq.(3.14), which is expressed by the Hadamard matrix of Eq.(3.2). The inner product of $\mathbf{a}^{m,\tau}$ and $\mathbf{a}^{m'}$ is written as

$$\begin{aligned}(\mathbf{a}^{m,\tau}, \mathbf{a}^{m'}) &= \sum_{n=0}^{N-1} \omega^{\tau n} a_n^m a_n^{m'} \\ &= \sum_{n=0}^{N/2-1} h_{m,n} h_{m',n} (\omega^{n\tau} + \omega^{N/2+n\tau}) \\ &= \begin{cases} N & \text{for } \tau = 0,\ m = m', \\ 0 & \text{for } \tau \neq 0,\ m = m', \\ 0 & \text{for } \tau = 0, \pm 1,\ m \neq m', \end{cases} \end{aligned} \tag{3.26}$$

since $\omega^{n\tau} + \omega^{N/2+n\tau} = 0$ for delay $\tau = \pm 1$, and

$$\sum_{n=0}^{N-1} \omega^{n\tau} = \begin{cases} N & \text{for } \tau = 0, \\ 0 & \text{for } \tau \neq 0\ . \end{cases} \tag{3.27}$$

Consequently, the orthogonality between ZCZ sequence $\mathbf{a}^{m'}$ and a frequency domain sequence $\mathbf{a}^{m,\tau}$, which is transformed from phase-shifted time domain sequence $\mathbf{s}^{m,\tau}$ with $|\tau| \leq 1$ by DFT, are maintained. It means that ZCZ code with Zcz=1 used in CDMA schemes can keep the orthogonality of the transmitted and received signal even the signal affected by multipath fading channel with one chip delay. Thus, by using ZCZ code, the ISI, ICI and MAI can be removed for one chip delay.

From the correlation properties of ZCZ code of Eq. (3.11), a binary matrix defined by

$$A = \begin{pmatrix} a_0^1 & a_1^1 & a_2^1 & \cdots & a_{N-1}^1 \\ a_0^2 & a_1^2 & a_2^2 & \cdots & a_{N-1}^2 \\ \vdots & \vdots & \vdots & \cdots & \vdots \\ a_0^{N/2} & a_1^{N/2} & a_2^{N/2} & \cdots & a_{N-1}^{N/2} \\ a_1^1 & a_2^1 & a_3^1 & \cdots & a_0^1 \\ a_1^2 & a_2^2 & a_3^2 & \cdots & a_0^2 \\ \vdots & \vdots & \vdots & \cdots & \vdots \\ a_1^{N/2} & a_2^{N/2} & a_3^{N/2} & \cdots & a_0^{N/2} \end{pmatrix} \tag{3.28}$$

is an orthogonal matrix [25]. Furthermore, from Eq.(3.26), a complex matrix defined

by

$$A = \begin{pmatrix} a_0^1 & a_1^1 & a_2^1 & \cdots & a_{N-1}^1 \\ a_0^2 & a_1^2 & a_2^2 & \cdots & a_{N-1}^2 \\ \vdots & \vdots & \vdots & \cdots & \vdots \\ a_0^{N/2} & a_1^{N/2} & a_2^{N/2} & \cdots & a_{N-1}^{N/2} \\ a_1^1 & \omega^1 a_2^1 & \omega^2 a_3^1 & \cdots & \omega^{N-1} a_0^1 \\ a_1^2 & \omega^1 a_2^2 & \omega^2 a_3^2 & \cdots & \omega^{N-1} a_0^2 \\ \vdots & \vdots & \vdots & \cdots & \vdots \\ a_1^{N/2} & \omega^1 a_2^{N/2} & \omega^2 a_3^{N/2} & \cdots & \omega^{N-1} a_0^{N/2} \end{pmatrix} \tag{3.29}$$

is also a complex Hadamard matrix (unitary matrix).

3.2 DS-ZCZ-CDMA Schemes and Their Problem

In this subsection, DS-ZCZ-CDMA and block coding (BC) DS-ZCZ-CDMA without MAI called BC-DS-ZCZ-CDMA are introduced and reviewed. Their problem in high data rate transmission is depicted.

3.2.1 DS-ZCZ-CDMA

This subsection gives an introduction to the fundamentals of DS-CDMA using ZCZ code [22], [24], which may be applied to quasi-synchronous systems. In these quasi-synchronous systems, the asynchronous mode is applied when there is a need to maintain the relative synchronicity in the time delay between the different users at the transmitter.

In DS-ZCZ-CDMA, a ZCZ code with length $N + N_g$ which is made by adding GI length $N_g = 2$ to the head and tail of the sequence a^m in A of Eq.(3.1) is allocated for a single user m, and can be written as

$$\hat{a}^m = (a_{N-1}^m, a_0^m, a_1^m, \cdots, a_n^m, \cdots, a_{N-1}^m, a_0^m). \tag{3.30}$$

Where GI play a role of interference-free despreading operation with ZCZ sequence $a^{m'}$ for delayed waves at the receiver. That is even if a data bit changes, the periodic

correlation function keeps zero for delay $\tau \leq Zcz$. A ZCZ code with $Zcz = 1$ is chosen to maximize the number of multiple users given by Eq.(3.12), and its construction is shown in Figure 3.5.

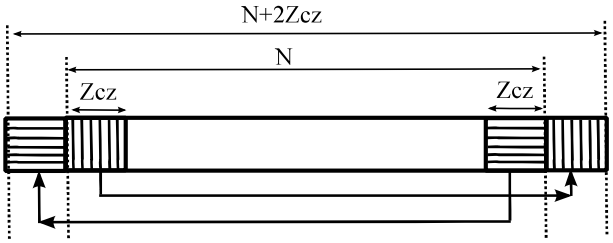

Figure 3.5: ZCZ sequence with GI ($Zcz = 1$)

Figure 3.6 illustrates a block digram of DS-ZCZ-CDMA for multiple users M.

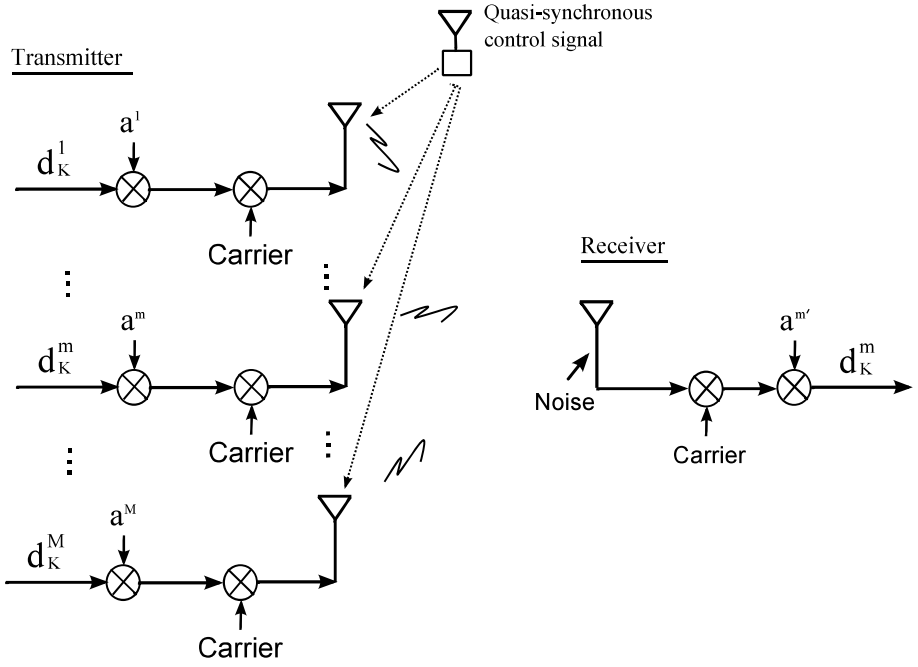

Figure 3.6: A basic model of DS-ZCZ-CDMA

At the transmitter, modulated data symbols $d_K^m \in C$ of mth user is first spreaded by a corresponding ZCZ sequence $\hat{a}^m$ with length $N + 2$, and transmitted after carrier frequency multiplication. The direct spreading process is shown in Figure 3.7. Moreover, each transmitter simultaneously sends the spread data symbol at a

timing designated by a timing control signal supplied by a control station.

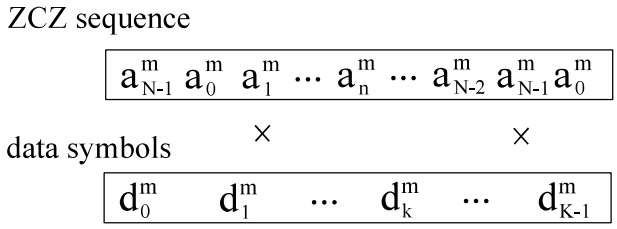

Figure 3.7: Spreading in DS-ZCZ-CDMA

At the receiver, the received signal consisting of symbols sent by M multiple users passed from multipath fading channel of Eq.(2.10) and added AWGN channel. A soft output to be used for detecting the transmitted data symbols, and the transmitted data symbols d^m_K is obtained by taking correlation (or inner product) between the received signal and a desired user sequence $a^{m'}$. The receiver may use the timing control signal to detect data frame synchronization quickly.

Figure 3.8 shows a basic concept of quasi-synchronous DS-ZCZ-CDMA for multiple access. By using the correlation properties of ZCZ code, the orthogonality between different users can be kept within allowed period or one chip delay.

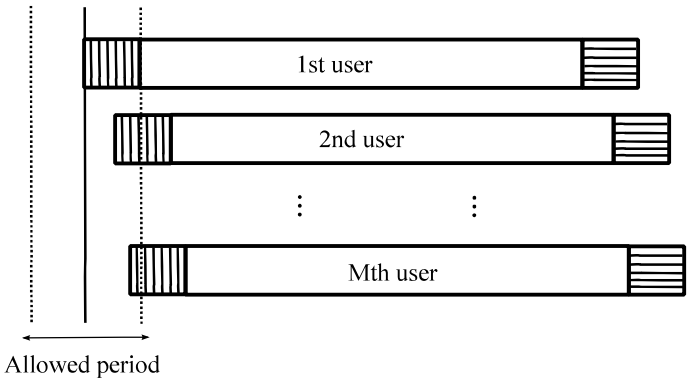

Figure 3.8: Quasi-synchronous DS-ZCZ-CDMA

3.2.2 BC-DS-ZCZ-CDMA

DS-ZCZ-CDMA can remove MAI and ISI in low data rate transmission with one chip delay spread. However, in high data rate transmission with large delay spread, the MAI and ISI are still induced and it will causes system performance degradation. To remove MAI, a block coding (BC) DS-ZCZ-CDMA scheme called BC-DS-ZCZ-CDMA based on a RAKE receiver utilizing the pilot sequence for channel estimation has been proposed [29]- [32].

Figure 3.9 illustrates the basic model of the BC-DS-ZCZ-CDMA for a single user m.

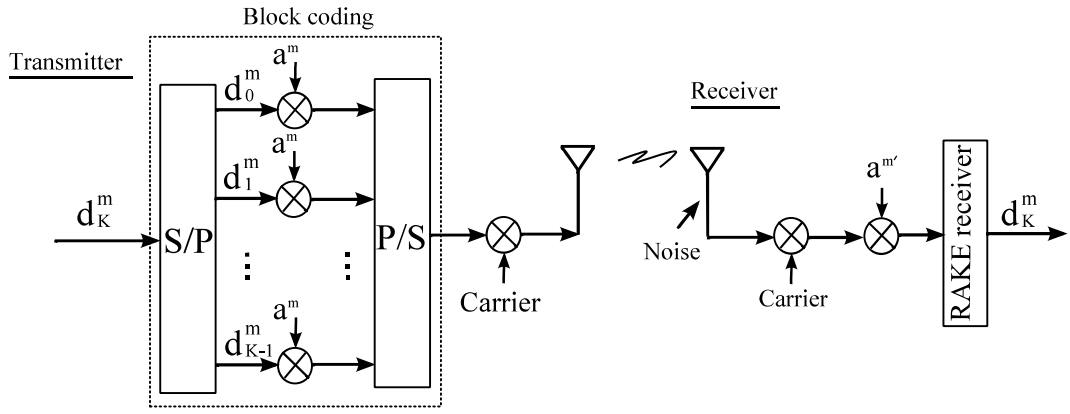

Figure 3.9: A basic model of BC-DS-ZCZ-CDMA

At the transmitter, the data symbols d_K^m of mth user is first spread by a ZCZ sequence with length $N+2$ after S/P conversion. Then a block coding technique is applied. The signal is transmitted after carrier frequency multiplication. The block coding technique is shown in Figure 3.10.

At the receiver, the received signal r^m consisting of symbols sent by M users with multipath fading and AWGN. A Rake receiver to be used for detecting the transmitted data symbols d_k^m. The d_k^m is obtained by taking correlation outputs (or inner product) between the received signal and a desired user sequence $a^{m'}$. The auto and cross-correlation function of ZCZ code applied block coding technique is shown in Figure 3.11. It can bee seen that by applying a block coding technique in DS-ZCZ-CDMA, MAI can be completely removed, since the Zcz is expanded K

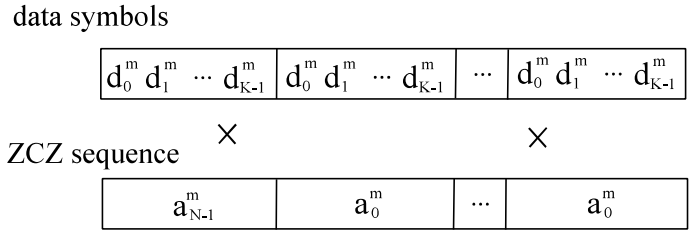

Figure 3.10: Block coding technique

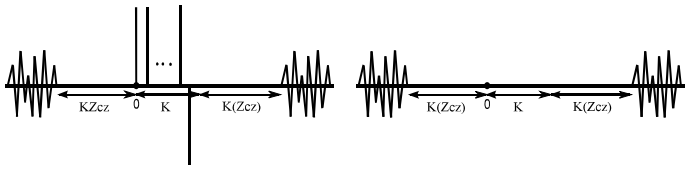

Figure 3.11: Auto and cross-correlation function of ZCZ code with block coding technique

time. However, ISI still exits.

Thus, the RAKE receiver utilizing the pilot sequence for channel estimation is applied to mitigate the influence of ISI. A pilot symbol sequence is added to the head of a transmitting data frame for frame synchronization or to recover the destroyed amplitude and phase oh the transmitted signal due to multipath. Transmission packet including data signal and pilot signal is shown in Figure 3.12.

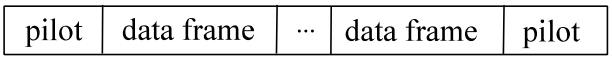

Figure 3.12: Transmission packet in BC-DS-ZCZ-CDMA

The pilot symbol sequence will be repeatedly transmitted several times to estimate the average signal levels in Figure 2.8. By using the average signal levels or impulse response of multipath channel which obtained by take a correlation between pilot signal and ZCZ sequence $a^{m'}$.

The received signal r^m can be expressed as

$$r^m = \begin{pmatrix} r_0^m \\ r_1^m \\ \vdots \\ r_k^m \\ \vdots \\ r_{K-1}^m \end{pmatrix} = \underbrace{\begin{pmatrix} p_0^m & 0 & \cdots & 0 & 0 & \cdots & 0 \\ p_1^m & p_0^m & \cdots & 0 & 0 & \cdots & 0 \\ \vdots & \vdots & \ddots & \vdots & \vdots & \ddots & \vdots \\ p_{J-1}^m & p_{J-2}^m & \cdots & p_0^m & 0 & \cdots & 0 \\ 0 & p_{J-1}^m & \cdots & p_1^m & p_0^m & \cdots & 0 \\ \vdots & \vdots & \ddots & \vdots & \vdots & \ddots & \vdots \\ 0 & 0 & \cdots & p_{J-1}^m & p_{J-2}^m & \cdots & p_0^m \\ \vdots & \vdots & \ddots & \vdots & \vdots & \ddots & \vdots \\ 0 & 0 & \cdots & 0 & 0 & \cdots & p_{J-2}^m \\ 0 & 0 & \cdots & 0 & 0 & \cdots & p_{J-1}^m \end{pmatrix}}_{P^m} \underbrace{\begin{pmatrix} d_0^m \\ d_1^m \\ \vdots \\ d_k^m \\ \vdots \\ d_{K-1}^m \end{pmatrix}}_{d^m} \tag{3.31}$$

where P^m is a $(K + J - 1) \times K$ matrix with J paths given by the levels of inner product output of a received pilot symbol sequence.

The data symbol sequence d_k^m of Eq. (3.31) can be detected by using a MMSE RAKE receiver

$$d^m = [P^m (P^m)^* + \sigma^2]^{-1} (P^m)^* r^m, \tag{3.32}$$

where $(.)^*$ denotes the complex conjugation transpose and $[.]^{-1}$ denotes the inverse of a matrix. In this dissertation, a MMSE RAKE receiver is applied, and it will be introduced in chapter 4 in detail.

Although BC-DS-ZCZ-CDMA has ability to completely remove MAI, but the ISI still exits. Moreover, as the increase of the size of transmitting data symbols, the system performance degrades [30], [56]. Thus, the single carrier BC-DS-ZCZ-CDMA scheme is not a promising technique for future high data rate transmission.

3.3 MC-ZCZ-CDMA without GI Technique and Its Problem

In this subsection, a general MC-CDMA using the above introduced ZCZ code with low correlation properties called MC-ZCZ-CDMA is presented. The ZCZ code can remove MAI, and mitigates the ISI and ICI for one chip delay. In general, in MC-CDMA, several chips (or GI) are added to the head and tail of time domain signal to prevent these interferences. However, the GI consumes additional transmission power. At the same time, in previous researches, a MC-ZCZ-CDMA scheme without GI has been considered to fully use the Zcz which related to the upper bound of ZCZ code by Eq.3.12 [46]- [48].

The block diagram of a general MC-ZCZ-CDMA without GI for multiple users M is shown in Figure 3.13. It is respectively referred to as the synchronous and quasi-synchronous transmissions in the cases of $\tau_m = 0$ and $|\tau_m - \tau_{m'}| \leq T_{delay}$ for any $m(\neq m')$, where τ_m denotes the delay time of a received signal of the mth user, and T_{delay} an allowable time delay.

At the transmitter, the kth data symbol $d_k^m \in C$ with $0 \leq k \leq K-1$ in one transmitting data frame of the mth user, is multiplied by a corresponding sequence a^m in the code A of Eq.(3.1). Through the S/P conversion, a frequency domain sequence is expressed by

$$\left.\begin{aligned} u_k^m = (u_{0,k}^m, u_{1,k}^m, \cdots, u_{n,k}^m, \cdots, u_{N-1,k}^m), \\ u_{n,k}^m = d_k^m a_n^m, \end{aligned}\right\} \tag{3.33}$$

where N is equal to the number of the subcarriers.

The frequency domain sequence u_k^m is converted into a time domain sequence

$$s_k^m = (s_{0,k}^m, s_{1,k}^m, \cdots, s_{q,k}^m, \cdots, s_{N-1,k}^m) \tag{3.34}$$

by the N-point IDFT of Eq.(3.22) given in the previous subsection.

After P/S conversion, the transmitting signal s^m can be expressed as

$$s^m(t) = \sqrt{\frac{2S}{N}} \sum_{q=0}^{N-1} s_{q,k}^m g(t - qT_c), \tag{3.35}$$

where T_c denotes the chip interval and S the average transmitting signal power.

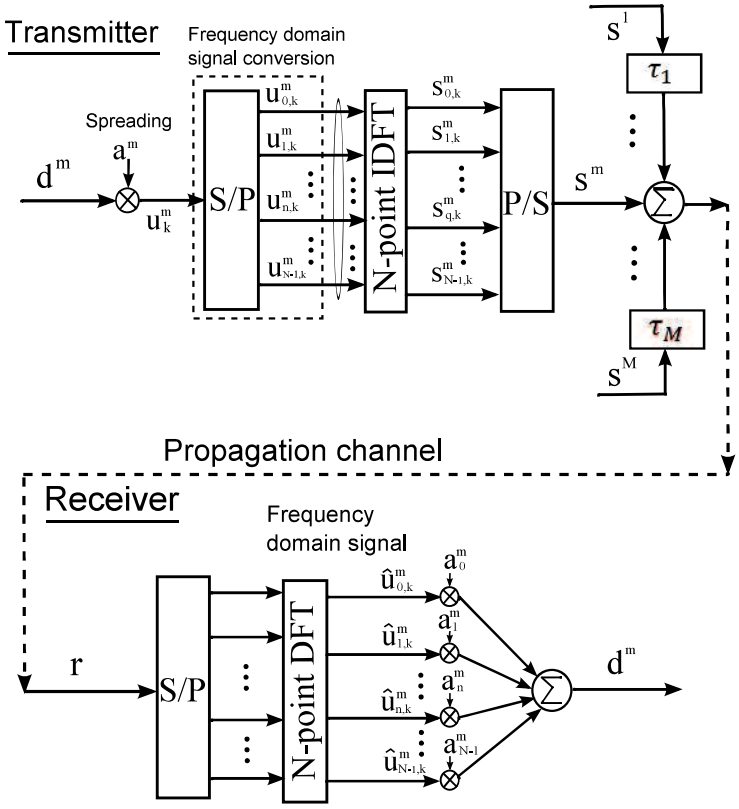

Figure 3.13: Block diagram of a general MC-ZCZ-CDMA without GI technique

The transmitting signal of the mth user of Eq.(3.35) is received as

$$\left.\begin{aligned} r(t) &= \sum_{m=0}^{M-1} r^m(t) + \eta(t), \\ r^m(t) &= \int_0^{\infty} p^m(\tau, t) s^m(t-\tau) d\tau \end{aligned}\right\} \tag{3.36}$$

through the multipath fading channel of Eqs. (2.10) and (2.11), where $\eta(t)$ is the AWGN.

The received signal $r(t)$ is converted into a discrete received signal by I/Q demodulator and low pass filter, and through S/P conversion, it is transformed into

$$\begin{aligned} r_{n,k} &= \sum_{m=0}^{M-1} \sum_{n=0}^{N-1} r^m(t) e^{\frac{-j2\pi(t-kT)n}{T_s}} \\ &= \sum_{m=0}^{M-1} \sqrt{\frac{2S}{N}} H_{n,k}^m u_{n,k}^m + \eta_{n,k} \end{aligned} \tag{3.37}$$

by the DFT. Where $T = T_s = NT_c$ and $\eta_{n,k}$ is the AWGN noise with zero-mean and a variance of $2N_0/T_s$, respectively.

Furthermore, the discrete symbol of Eq.(3.37) is equalized to mitigate the frequency distortion due to a multi-path fading. A MMSE Rake receiver is considered

since it exploits full frequency diversity among various equalization weights [5], and its detail will be presented in next chapter in depth. Finally, the received data symbol d^m is detected by using both inner product of special pilot symbols with sequence $a^{m'}$ and frequency domain signal $\hat{u}_k^m$ with sequence $a^{m'}$.

In high data rate transmission with large delay spread, the transmitted signal of Eq.(3.35) is arrived to the receiver with different time delay and multiple users. Thus, the received signal affected by ISI, ICI and MAI, and causes system performance deterioration.

Figures 3.14 shows the received signal with a single user for one chip delay as $\tau_1 = 1$. In this case, the ZCZ code can remove these interference within one chip delay with less data symbols K, however, as the K increases, the ZCZ code can not guarantee the Zcz and unable to remove these interferences, and induces system performance degradation.

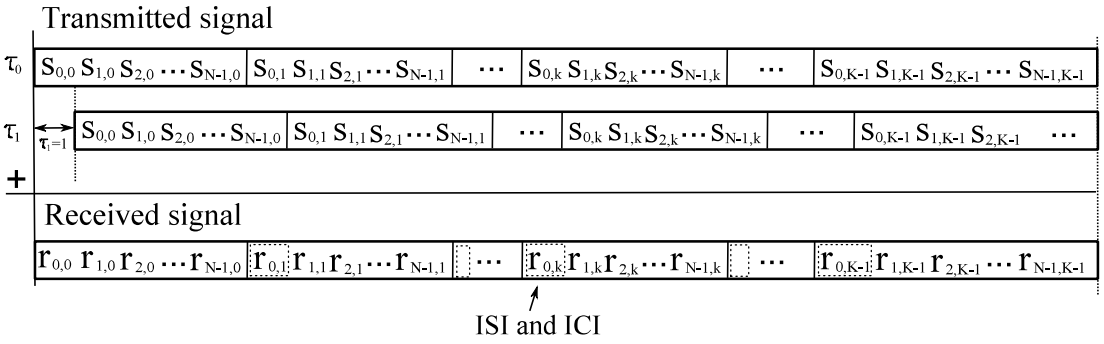

Figure 3.14: Received signal in one chip delay spread

By using a ZCZ code with wide Zcz given by Eq.(3.12), it is possible to combat one or more than one chip delay spread. However, there is a trade-off of the BER performance and the number of users, since the family size of ZCZ code decreases as the increases of Zcz.

Chapter4

MC-ZCZ-CDMA Schemes in Large Delay Spread

In this chapter, firstly, a general MC-ZCZ-CDMA scheme with GI technique is introduced. Then, a proposal block coding MC-ZCZ-CDMA scheme without interference called BC-MC-ZCZ-CDMA based on above general scheme is presented.

4.1 A Basic MC-ZCZ-CDMA with GI Technique

In this section, a general MC-ZCZ-CDMA scheme with GI technique in large delay spread or synchronization gaps of more than one chip is presented. The block diagram of a general MC-ZCZ-CMDA with GI technique used MMSE Rake receiver for a single user m is illustrated in Figure 4.1. For simplicity, a digital baseband is considered.

4.1.1 Transmitting System

At the transmitter, the complex kth data symbol $d_k^m \in C$ is multiplied by a corresponding sequence $\mathbf{a}^m$ in ZCZ code $A(N, N/2, 1)$, and through S/P conversion, a frequency domain sequence is expressed by

$$\left.\begin{aligned} \mathbf{u}_k^m = (u_{0,k}^m, u_{1,k}^m, \cdots, u_{n,k}^m, \cdots, u_{N-1,k}^m), \\ u_{n,k}^m = d_k^m a_n^m, \end{aligned}\right\} \tag{4.1}$$

where N is corresponding to the number of the subcarriers.

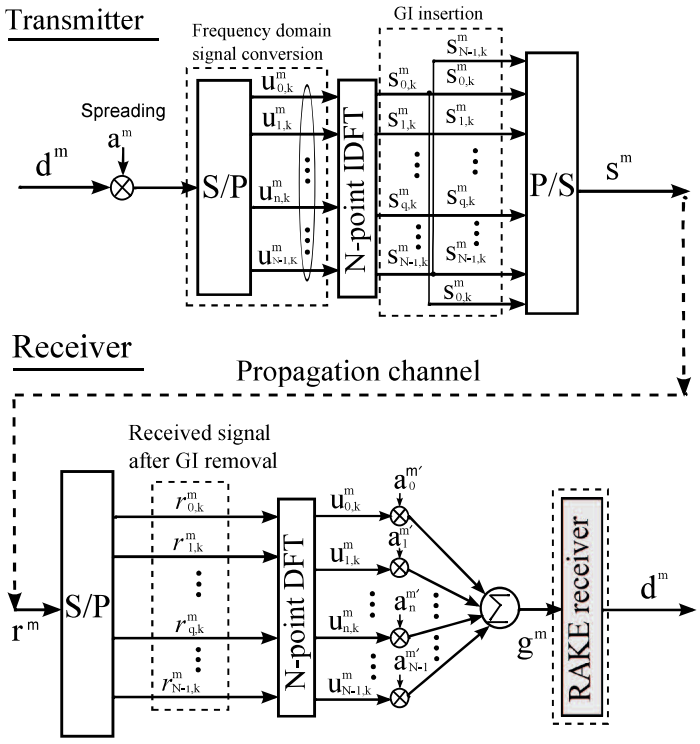

Figure 4.1: Basic model of a MC-ZCZ-CDMA with GI technique

The frequency domain sequence $\mathbf{u}_k^m$ is converted into a time domain sequence

$$\mathbf{s}_k^m = (s_{0,k}^m, s_{1,k}^m, \cdots, s_{q,k}^m, \cdots, s_{N-1,k}^m) \tag{4.2}$$

by the N-point IDFT of Eq.(3.22).

Let $\hat{\mathbf{s}}_k^m$ be an extended time domain sequence of length $\hat{N} = N + N_g$ with $N_g = 2$ by Eq.(3.30), which includes the GI of length N_g is added to $\mathbf{s}_k^m$ to prevent ICI, is written as

$$\begin{aligned} \hat{\mathbf{s}}_k^m &= (\hat{s}_{0,k}^m, \hat{s}_{1,k}^m, \cdots, \hat{s}_{q,k}^m, \cdots, \hat{s}_{\hat{N}-1,k}^m) \\ &= (s_{N-1,k}^m, s_{0,k}^m, \cdots, s_{q,k}^m, \cdots, s_{N-1,k}^m, s_{0,k}^m), \end{aligned} \tag{4.3}$$

where $\hat{s}_{q,k}^m = s_{(N-1+q)modN,k}^m$.

Let S^m be a data frame with GI, expressed by a $(N+2) \times K$ matrix

$$S^m = ((\hat{\mathbf{s}}_0^m)^T, (\hat{\mathbf{s}}_1^m)^T, \cdots, (\hat{\mathbf{s}}_k^m)^T, \cdots, (\hat{\mathbf{s}}_{K-1}^m)^T)$$

$$= \begin{pmatrix} s^m_{N-1,0} & \cdots & s^m_{N-1,k} & \cdots & s^m_{N-1,K-1} \\ s^m_{0,0} & \cdots & s^m_{0,k} & \cdots & s^m_{0,K-1} \\ s^m_{1,0} & \cdots & s^m_{1,k} & \cdots & s^m_{1,K-1} \\ \vdots & & \vdots & & \vdots \\ s^m_{q,0} & \cdots & s^m_{q,k} & \cdots & s^m_{q,K-1} \\ \vdots & & \vdots & & \vdots \\ s^m_{N-1,0} & \cdots & s^m_{N-1,k} & \cdots & s^m_{N-1,K-1} \\ s^m_{0,0} & \cdots & s^m_{0,k} & \cdots & s^m_{0,K-1} \end{pmatrix}, \tag{4.4}$$

where $(.)^T$ denotes the transpose of a matrix.

After the P/S conversion, the data frame of length $K\hat{N}$ is written as

$$\begin{aligned} \mathbf{s}^m = (&s^m_{N-1,0}, s^m_{0,0}, s^m_{1,0}, \cdots, s^m_{q,0}, \cdots, s^m_{N-1,0}, s^m_{0,0}, \cdots, \\ &s^m_{N-1,k}, s^m_{0,k}, s^m_{1,k}, \cdots, s^m_{q,k}, \cdots, s^m_{N-1,k}, s^m_{0,k}, \cdots, \\ &s^m_{N-1,K-1}, s^m_{0,K-1}, s^m_{1,K-1}, \cdots, s^m_{q,K-1}, \cdots, s^m_{N-1,K-1}, s^m_{0,K-1}). \end{aligned} \tag{4.5}$$

The transmitting signal of Eq.(4.5) may travel through different propagation paths Eq.(2.10) and arrive at the receiver with different delays as shown in Figure 2.7. These time-dispersive paths may cause the interferences ISI, ICI and MAI.

4.1.2 Receiving System

At the receiver, the set of the received data frames except N_g is expressed by a $N \times K$ matrix

$$\begin{aligned} r^m &= ((\mathbf{r}^m_0)^T, (\mathbf{r}^m_1)^T, \cdots, (\mathbf{r}^m_k)^T, \cdots, (\mathbf{r}^m_{K-1})^T) \\ &= \begin{pmatrix} r^m_{0,0} & \cdots & r^m_{0,k} & \cdots & r^m_{0,K-1} \\ r^m_{1,0} & \cdots & r^m_{1,k} & \cdots & r^m_{1,K-1} \\ \vdots & & \vdots & & \vdots \\ r^m_{q,0} & \cdots & r^m_{q,k} & \cdots & r^m_{q,K-1} \\ \vdots & & \vdots & & \vdots \\ r^m_{N-1,0} & \cdots & r^m_{N-1,k} & \cdots & r^m_{N-1,K-1} \end{pmatrix}. \end{aligned} \tag{4.6}$$

Figures 4.2 and 4.3 show the received signal r^m and the transmitting data symbols d_k in one or more than one chip delay spread. For $\tau_1 = 1$ chip delay, ISI and ICI

does not occur. However, for $\tau_2 = 2$ chips delay, ISI ans ICI occur, because the orthogonality of the subcarriers is destroyed. Otherwise, MAI induces the system performance degradation.

Figure 4.2: Received signal in large delay spread

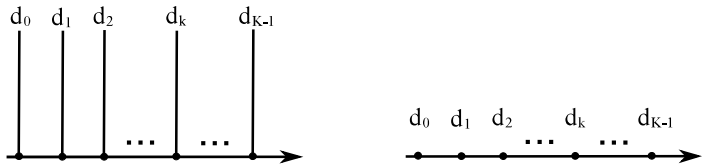

(a) Innner products of single and multiple users with one chip delay

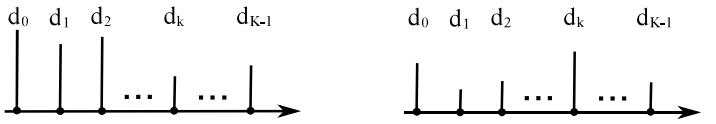

(b) Innner products of single and multiple users with large delay

Figure 4.3: Values of transmitting data symbols

Finally, the received symbols $\mathbf{r}_k^m$ is transformed into the frequency domain $\mathbf{u}_k^m$ by using N-point DFT, and the average pilot symbol levels $\mathbf{p}^m$ relating to the Eq.(2.12) is equal to the inner product output of the received pilot symbol sequence and ZCZ sequence a^m. A MMSE RAKE receiver utilizing the pilot sequence for channel estimation is applied for frame synchronization or equalization, and its detail will be explained in section 4.2.

4.2 BC-MC-ZCZ-CDMA

In this section, a novel BC-MC-ZCZ-CDMA without interferences based on the MC-ZCZ-CDMA with GI technique in large delay spread or synchronization gaps of more than one chip is presented by utilizing the correlation properties of Eq.(3.26) [55], [56]. Also, the digital baseband is considered for simplicity.

4.2.1 Basic Model

Figure 4.4 illustrates the basic model of BC-MC-ZCZ-CDMA, which uses a block coding technique and the MMSE RAKE receiver utilizing the pilot sequence for channel estimation.

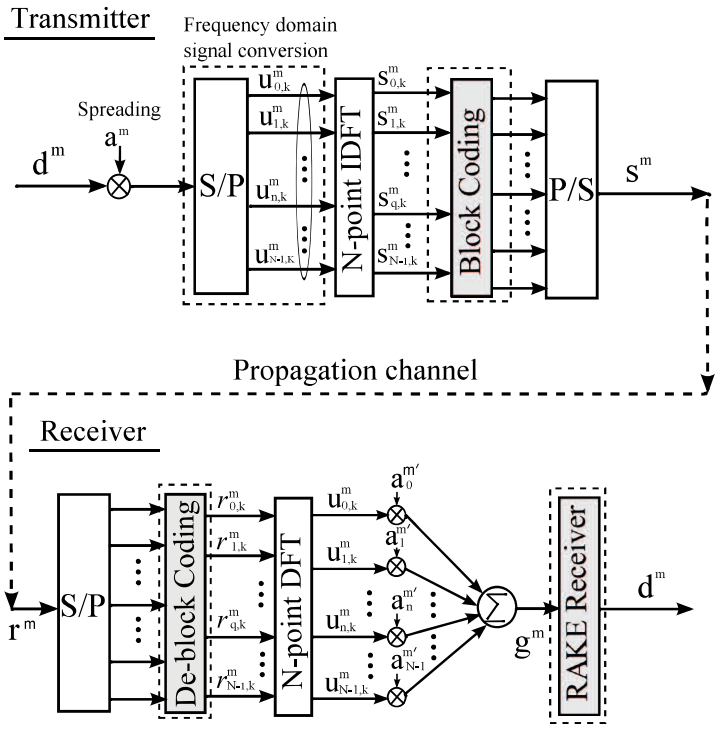

Figure 4.4: Basic model of BC-MC-ZCZ-CDMA

4.2.2 Transmitting System

At a transmitter, let $\mathbf{d}^m$ be a sequence of K data symbols of the mth user written as

$$\mathbf{d}^m = (d_0^m, d_1^m, \cdots, d_k^m \cdots, d_{K-1}^m), \quad d_k^m \in C, \tag{4.7}$$

where C denotes a set of complex numbers and K means a block size.

The kth data symbol d_k^m is multiplied by a corresponding sequence $\mathbf{a}^m$ in ZCZ code $A(N, N/2, 1)$, and through the S/P conversion, a frequency domain sequence is expressed by

$$\left.\begin{aligned} \mathbf{u}_k^m &= (u_{0,k}^m, u_{1,k}^m, \cdots, u_{n,k}^m, \cdots, u_{N-1,k}^m), \\ u_{n,k}^m &= d_k^m a_n^m, \end{aligned}\right\} \tag{4.8}$$

where N is corresponding to the number of the subcarriers.

The frequency domain sequence $\mathbf{u}_k^m$ is converted into a time domain sequence

$$\mathbf{s}_k^m = (s_{0,k}^m, s_{1,k}^m, \cdots, s_{q,k}^m, \cdots, s_{N-1,k}^m) \tag{4.9}$$

by the N-point IDFT of Eq.(3.22).

Let $\hat{\mathbf{s}}_k^m$ be an extended time domain sequence of length $\hat{N} = N + N_g$ with $N_g = 2$, which includes the GI of length N_g is added to $\mathbf{s}_k^m$ to prevent ICI, is written as

$$\begin{aligned} \hat{\mathbf{s}}_k^m &= (\hat{s}_{0,k}^m, \hat{s}_{1,k}^m, \cdots, \hat{s}_{q,k}^m, \cdots, \hat{s}_{\hat{N}-1,k}^m) \\ &= (s_{N-1,k}^m, s_{0,k}^m, \cdots, s_{q,k}^m, \cdots, s_{N-1,k}^m, s_{0,k}^m), \end{aligned} \tag{4.10}$$

where $\hat{s}_{q,k}^m = s_{(N-1+q) mod N,k}^m$.

Let S^m be a data frame constructed by a block coding technique referred to an interleaving method, expressed by a $(N+2) \times K$ matrix

$$\begin{aligned} S^m &= ((\hat{\mathbf{s}}_0^m)^T, (\hat{\mathbf{s}}_1^m)^T, \cdots, (\hat{\mathbf{s}}_k^m)^T, \cdots, (\hat{\mathbf{s}}_{K-1}^m)^T) \\ &= \begin{pmatrix} s_{N-1,0}^m & \cdots & s_{N-1,k}^m & \cdots & s_{N-1,K-1}^m \\ s_{0,0}^m & \cdots & s_{0,k}^m & \cdots & s_{0,K-1}^m \\ s_{1,0}^m & \cdots & s_{1,k}^m & \cdots & s_{1,K-1}^m \\ \vdots & & \vdots & & \vdots \\ s_{q,0}^m & \cdots & s_{q,k}^m & \cdots & s_{q,K-1}^m \\ \vdots & & \vdots & & \vdots \\ s_{N-1,0}^m & \cdots & s_{N-1,k}^m & \cdots & s_{N-1,K-1}^m \\ s_{0,0}^m & \cdots & s_{0,k}^m & \cdots & s_{0,K-1}^m \end{pmatrix}, \end{aligned} \tag{4.11}$$

where $(.)^T$ denotes the transpose of a matrix.

After the P/S conversion, the data frame of length $K\hat{N}$ is written as

$$\begin{aligned}\mathbf{s}^m = (&s^m_{N-1,0}, \cdots, s^m_{N-1,k} \cdots, s^m_{N-1,K-1},\\ &s^m_{0,0}, \cdots, s^m_{0,k}, \cdots, s^m_{0,K-1}, \cdots,\\ &s^m_{N-1,0}, \cdots, s^m_{N-1,k}, \cdots, s^m_{N-1,K-1},\\ &s^m_{0,0}, \cdots, s^m_{0,k}, \cdots, s^m_{0,K-1}).\end{aligned} \tag{4.12}$$

4.2.3 Receiving System

At a receiver, the set of the received data frames except N_g is expressed by a $N \times K$ matrix

$$\begin{aligned} r^m &= ((\mathbf{r}^m_0)^T, (\mathbf{r}^m_1)^T, \cdots, (\mathbf{r}^m_k)^T, \cdots, (\mathbf{r}^m_{K-1})^T)\\ &= \begin{pmatrix} r^m_{0,0} & \cdots & r^m_{0,k} & \cdots & r^m_{0,K-1} \\ r^m_{1,0} & \cdots & r^m_{1,k} & \cdots & r^m_{1,K-1} \\ \vdots & & \vdots & & \vdots \\ r^m_{q,0} & \cdots & r^m_{q,k} & \cdots & r^m_{q,K-1} \\ \vdots & & \vdots & & \vdots \\ r^m_{N-1,0} & \cdots & r^m_{N-1,k} & \cdots & r^m_{N-1,K-1} \end{pmatrix}. \end{aligned} \tag{4.13}$$

Let L be the maximum of delay chips defined by $L = \tau_{J-1}$ with $\tau_0 = 0$. In this paper, the maximum L is settled within block length K ($L \leq K$). The received signal $\mathbf{r}^m_k$ with l ($0 \leq l \leq L$) chip delay can be written as

$$\mathbf{r}^m_k = \sum_{l=0}^{k} p^m_l \mathbf{s}^m_{k-l} + \sum_{l=0}^{L-k} p^m_{l+k-1} \mathbf{s}^{m,\tau}_{k-1-l} + \mathbf{n}, \tag{4.14}$$

where the first term except $l = 0$ represents ISI and second term represents ICI, and $\mathbf{n}$ is the AWGN with a single sided power spectral density of N_0 defined by

$$\mathbf{n} = (n_0, n_1, \cdots, n_k, \cdots, n_{K-1}). \tag{4.15}$$

Figure 4.5 shows the received signal r^m in large delay spread. It can be seen that the ICI and MAI are free for the delay length L shorter than the block side K.

The received symbols $\mathbf{r}^m_k$ are transformed into the frequency domain $\mathbf{u}^m_k$ by using N-point DFT

$$\mathbf{u}^m_k = \sum_{l=0}^{k} p^m_l d^m_{k-l} \mathbf{a}^m + \sum_{l=0}^{L-k} p^m_{l+k-1} d^m_{k-1-l} \mathbf{a}^m + \mathbf{n}. \tag{4.16}$$

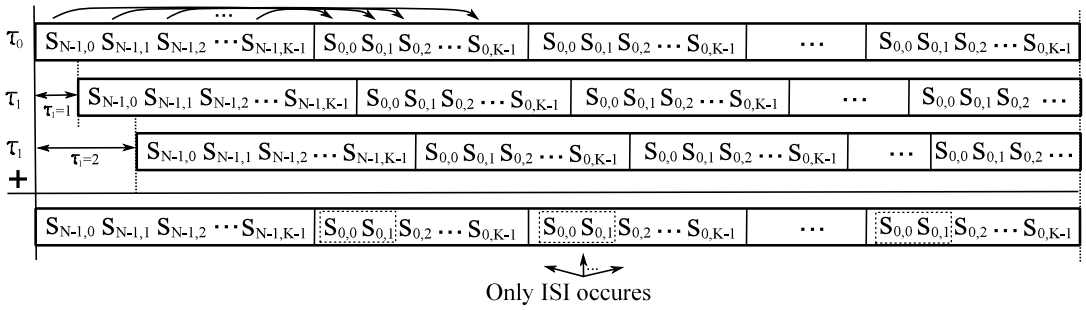

Figure 4.5: Received signal of BC-MC-ZCZ-CDMA in large delay spread

The inner product g_k^m between $\mathbf{u}_k^m$ and $\mathbf{a}^{m'}$ expressed by

$$\begin{aligned} g_k^m &= (\mathbf{u}_k^m, \mathbf{a}^{m'}) \\ &= \sum_{l=0}^{k-1} p_l^m d_{k-l}(\mathbf{a}^{m,\tau}, \mathbf{a}^{m'}) + \sum_{l=0}^{L-k} p_{l+k-1}^m d_{k-1-l}(\mathbf{a}^{m,\tau}, \mathbf{a}^{m'}) + (\mathbf{n}, \mathbf{a}^{m'}) \\ &= \begin{cases} N\sum_{l=0}^{k} p_l^m d_{k-l} + \hat{n} & \text{for } m = m', \\ \hat{n} & \text{for } m \neq m' \ , \end{cases} \end{aligned} \tag{4.17}$$

where $\hat{n} = (\mathbf{n}, \mathbf{a}^{m'})$.

Note that MAI and ICI are free from Eq.(4.17) drived from Eq.(3.26). However, ISI still exists and it influences the system performance.

The relation between the received data symbol sequence $\mathbf{g}^m$ of length $K + J - 1$ expressed by

$$\mathbf{g}^m = (g_o^m, g_1^m, \cdots, g_k^m, \cdots, g_{K+J-1}^m)^T \tag{4.18}$$

and the data symbol sequence $\mathbf{d}^m$ of length K of Eq.(4.7) is written as

$$\mathbf{g}^m = P^m(\mathbf{d^m})^T, \tag{4.19}$$

where P^m is a $(K+J-1)\times K$ matrix consisting of signal levels of Eq.(2.12) expressed

as

$$P^m = \begin{pmatrix} p_0^m & 0 & \cdots & 0 & 0 & \cdots & 0 \\ p_1^m & p_0^m & \cdots & 0 & 0 & \cdots & 0 \\ \vdots & \vdots & \ddots & \vdots & \vdots & \ddots & \vdots \\ p_{J-1}^m & p_{J-2}^m & \cdots & p_0^m & 0 & \cdots & 0 \\ 0 & p_{J-1}^m & \cdots & p_1^m & p_0^m & \cdots & 0 \\ \vdots & \vdots & \ddots & \vdots & \vdots & \ddots & \vdots \\ 0 & 0 & \cdots & p_{J-1}^m & p_{J-2}^m & \cdots & p_0^m \\ \vdots & \vdots & \ddots & \vdots & \vdots & \ddots & \vdots \\ 0 & 0 & \cdots & 0 & 0 & \cdots & p_{J-2}^m \\ 0 & 0 & \cdots & 0 & 0 & \cdots & p_{J-1}^m \end{pmatrix}. \tag{4.20}$$

In fact, to cancel the influence of a synchronization gap w chip, data symbols may include w dummy data symbols, and be written as

$$d_{K-w-1} = d_{K-w} = \cdots = d_{K-1} = 0. \tag{4.21}$$

The data symbol sequence $\mathbf{d}^m$ can be detected by using the MMSE RAKE receiver

$$\mathbf{d}^m = [P^m (P^m)^* + \sigma^2 I]^{-1} (P^m)^* \mathbf{g}^m, \tag{4.22}$$

where $(.)^*$ denotes the complex conjugation transpose, $[.]^{-1}$ denotes the inverse of a matrix, σ^2 is the accurate noise power, and I is a unit matrix used to keep the tetragonality of the matrix.

The Rake receiver with pilot-symbol-aided channel estimation is applied to mitigate the influence of ISI and achieves high frequency diversity. A pilot symbol sequence is added to the head of a transmitting data frame for frame synchronization or equalization.

To discuss simply, let us consider a pilot symbol sequence $\mathbf{s}_p^m$ of length $K(N+2)$, written as

$$\mathbf{s}_p^m = (s_{p_{N-1,0}^m}, 0, \cdots, 0, s_{p_{0,0}^m}, 0, \cdots, 0, \cdots, s_{p_{0,k}^m}, 0, \cdots, \cdots, 0, s_{p_{0,0}^m}, 0, \cdots, 0), \tag{4.23}$$

where $s_{p_{q,0}^m} = s_{q,0}^m$ with $d_k^m = 1$ and $s_{p_{q,k}^m} = 0$ with $d_k^m = 1$ for $1 \leq k \leq K-1$ in Eq.(4.12).

Figure 4.6 shows the transmitting data symbols d_k in large delay spread. It can be seen that the ICI and MAI are free for the delay length L shorter than the block side K.

Figure 4.6: Values of transmitting data symbols

Thus, by applying a block coding technique in MC-ZCZ-CDMA, an interference free system can be implemented. As a result, it is expected that the proposed scheme is applicable for a high data rate transmission with large delay spread. In order to verify the effectiveness of the proposed scheme in large delay spread, a computer simulation and evaluation will be given in chapter 5.

Chapter5

Simulation and Evaluation

In this chapter, the improved BER performance of the proposal BC-MC-ZCZ-CDMA scheme comparing with conventional ZCZ-CDMA schemes in large delay spread is demonstrated by computer simulation. First, the simulation conditions or parameters are given. Then, the simulation results are shown and analized. Finally, the effectiveness of proposed scheme is presented.

5.1 Simulation Condition

In order to evaluate the effectiveness of four kinds of orthogonal codes such as GO, EO, GZCZ and EZCZ introduced in Chapter 3 for MC-CDMA, a computer simulation is applied. Because of an orthogonal code with low correlation property may mitigate these interferences for large delay spread $\tau_j > 0$ in Figure 2.7. A synchronous transmission is assumed and QPSK modulation is applied. The number of multiple users $M = 4$, transmitting data symbols $K = 64$, code length $N = 64$. The number of subcarriers equals the code length N. To discuss simply and clearly, it is assumed that two-paths Rayleigh fading channel with an equal-power delay profile, i.e., decay factor $\alpha = 0$ by Eq.(2.13). The first and second path's delay spread is settled as $\tau_0 = 0$ and $T_c \leq \tau_1 \leq 16T_c$ by Eq.(2.12), where in the case of considering delay spread chip L, it is defined as $L = \tau_j/T_c$. The MMSE equalization is applied and channel estimation is considered to be ideal.

The above simulation parameters are used to evaluate the BER performance of

orthogonal codes, and its results are shown in Figures 5.1 and 5.2.

Moreover, in order to demonstrate the improved BER performance of MC-BC-ZCZ-CDMA comparing with conventional ZCZ-CDMA schemes in quasi-synchronous communications, a computer simulation is applied. QPSK and 16QAM modulation schemes are applied and the EZCZ code with length $N = 8, 16, 32$ and 64 is used as a spreading code. The block size or number of transmitting data symbols $K = 8$ and 16. Length of GI is settled as $N_g = 2$ chips, and number of subcarriers is N. Number of multiple access users are $M = 4$. It is assumed that two-paths Rayleigh fading channel with an equal-power delay profile, i.e., decay factor $\alpha = 0$ by Eq.(2.13). The length of large delay spread is settled as $L \leq K$. A MMSE Rake receiver is applied and channel estimation is considered to be ideal. The simulation parameters are listed in Table 5.1.

Table 5.1: Simulation parameters

Communication technique	quasi-synchronous communication
Data modulation	QPSK, 16QAM
Spreading code	EZCZ code (N, N/2, 1)
Code length	$N = 8, 16, 32, 64$
Block size	$K = 8, 16$
Length of GI	$N_g = 2$
No. of subcarriers	N
No. of multiple users	$M = 4$
Channel model	two-paths equal-power delay profile with $\alpha = 0$
Delay spread	$L = \tau_{J-1}$ with $\tau_0 = 0$ (chips)
Equalization technique	MMSE Rake receiver
Channel estimation	Ideal

The above simulation parameters are used to evaluate the BER performance of proposed scheme, and its results are shown in Figures 5.3, 5.4, 5.5, 5.6, 5.7, 5.8, 5.10 and 5.11, respectively.

5.2 Results and Comparison

Figure 5.1 shows the BER versus delay spread $0 \leq L \leq 16$ chips for the energy per bit to noise power spectral density ratio $E_b/N_0 = 20$ dB in synchronous MC-CDMA with QPSK modulation. It is observed that the BER performance of any orthogonal code is the same at $L = 0$, that of ZCZ codes is also the same at $L = 1$ chip. However, as the L increase, the BER performance of all codes deceases. But the EZCZ code provides the best BER performance, since it possess low correlation properties.

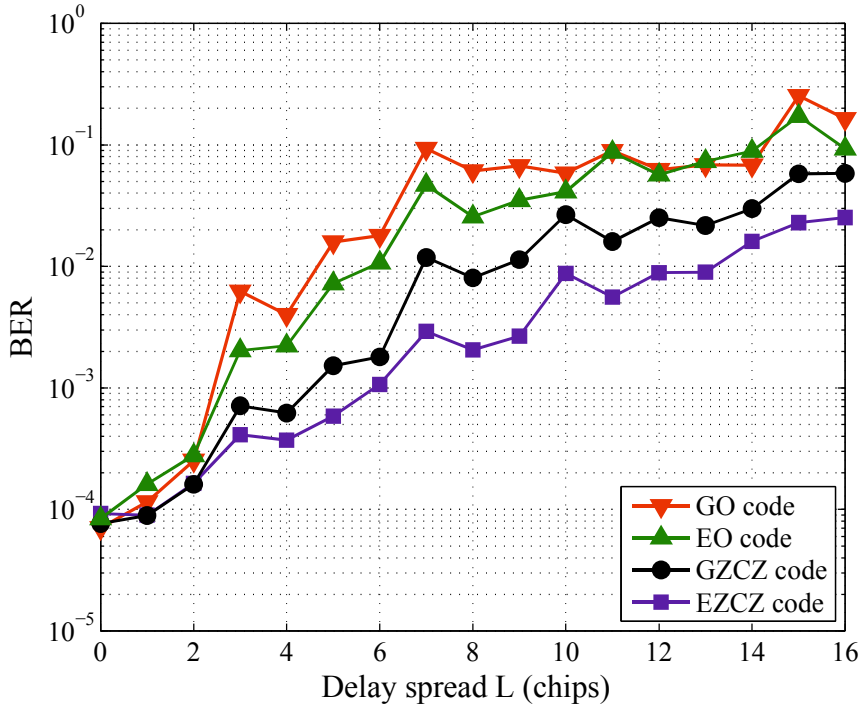

Figure 5.1: BER performance of four kinds of orthogonal codes in large delay spread

Figure 5.2 shows the BER versus E_b/N_o for delay spread $L = 4$ chips in synchronous MC-CDMA with QPSK modulation. It is confirmed that EZCZ code provides the best BER performance. At the same time, the BER performance of GZCZ code is almost same with EZCZ code. However, as the increasing of the length of delay spread L, the BER performance of GO and EO code drastically decreases. Thus, the EZCZ code with low correlation properties can be applicable for multicarrier CDMA in high data rate transmission with large delay spread, since

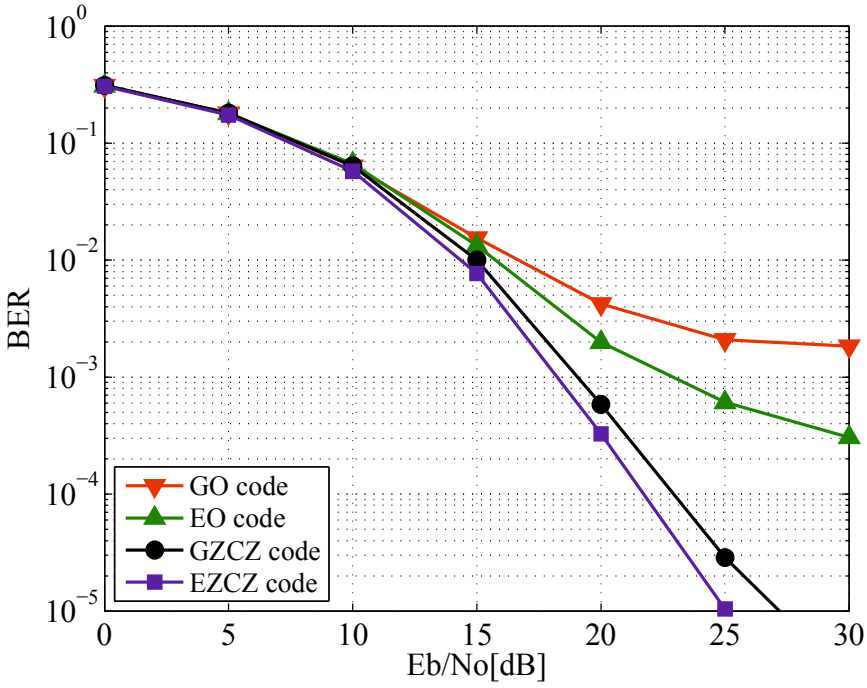

Figure 5.2: BER performance of four kinds of orthogonal codes in large delay spread

it has ability to mitigate these interferences.

Figure 5.3 shows the BER performance of the conventional MC-CDMA for single access with $M = 1$ user in large delay spread with the maximum of delay spread $L = 5$ chips to examine the influence of ISI and ICI. In MC-CDMA, ZCZ codes $A(N, M, Zcz)$ with $N = 32$, $M = N/(2 \times Zcz)$, $Zcz = 1, 2, 4$ or 8 and an orthogonal code (Hadamard matrix) given by Eq.(3.2) are used, the kth data symbol of the mth user of Eq.(4.9) is directly transmitted without adding guard chips, and the MMSE RAKE receiver and frequency domain equalization techniques are used to obtain good performance. The proposed scheme using $A(32, 16, 1)$ does not catch the influence of ISI and ICI, but the conventional schemes greatly do if $L > Zcz$, and family size decreases extremely. The BER performance of MC-CDMA using ZCZ code $A(32, 16, 1)$ is worse than that of the proposed scheme since the influence of ISI and ICI exists even if $L < Zcz$, since guard chips are not added.

Similarly, Figure 5.4 shows the BER performance over a two-path equal power delay profile for multiple access with QPSK for multiple users $M = 4$. It can be confirmed that BC-MC-ZCZ-CDMA is free from MAI, even if multiple users $M > 4$.

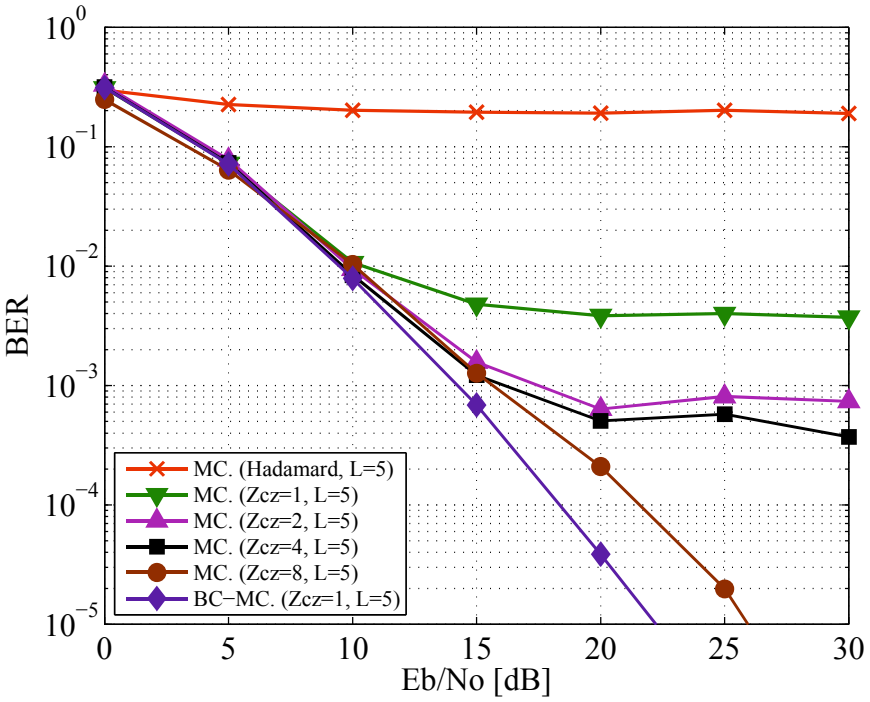

Figure 5.3: BER performance of MC-CDMA and BC-MC-ZCZ-CDMA with QPSK in large delay spread ($M = 1$, $N = 32$)

But in MC-CDMA, the influence of MAI becomes larger for delay spread $L > Zcz$.

Figure 5.5 shows the BER performance of BC-MC-ZCZ-CDMA with QPSK over a two-path equal power delay profile with delay spread $L = 4$ and 9 for code length N and block size K. It is shown that the BER performance of proposed scheme with code length $N = 16, 32$ and 64 is almost the same for $L \leq K$. It is confirmed that the BER performance of the proposed scheme with code length $N = 8$ is improved approximately 6 dB for $BER = 10^{-4}$ in comparison with $N = 16, 32$ and 64. Moreover, for $L \leq K$, the BER performance is almost the same. However, for $L > K$, the BER performance is drastically decreased.

Figure 5.6 shows the BER versus delay spread L for $E_b/N_0 = 12$ dB in BC-MC-ZCZ-CDMA with QPSK . It is clarified that the delay spread L does not affect the system performance if L does not exceed K. The capability of fighting against interference improves as code length N increases when delay spread L exceeds block size K. For code length $N = 8$, the graph of BER for length of delay chips fluctuates.

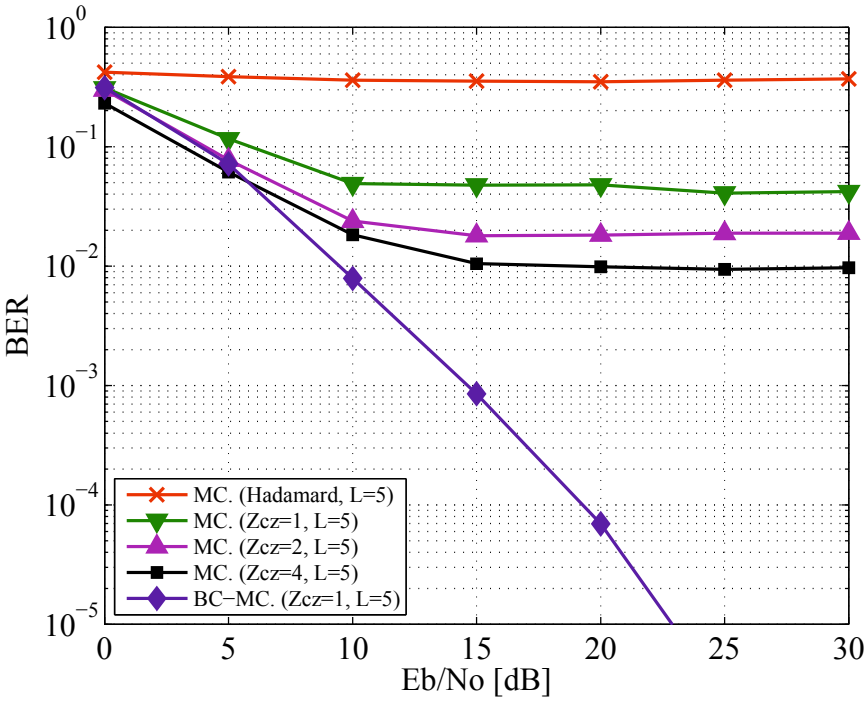

Figure 5.4: BER performance of MC-CDMA and BC-MC-ZCZ-CDMA with QPSK in large delay spread ($M = 4$, $N = 32$)

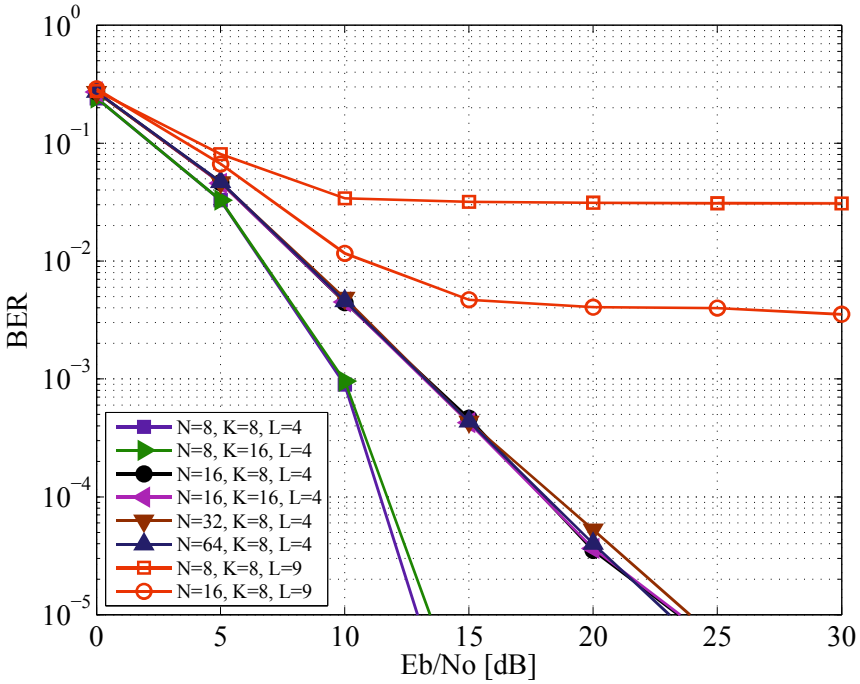

Figure 5.5: BER performance of BC-MC-ZCZ-CDMA with QPSK for N and K

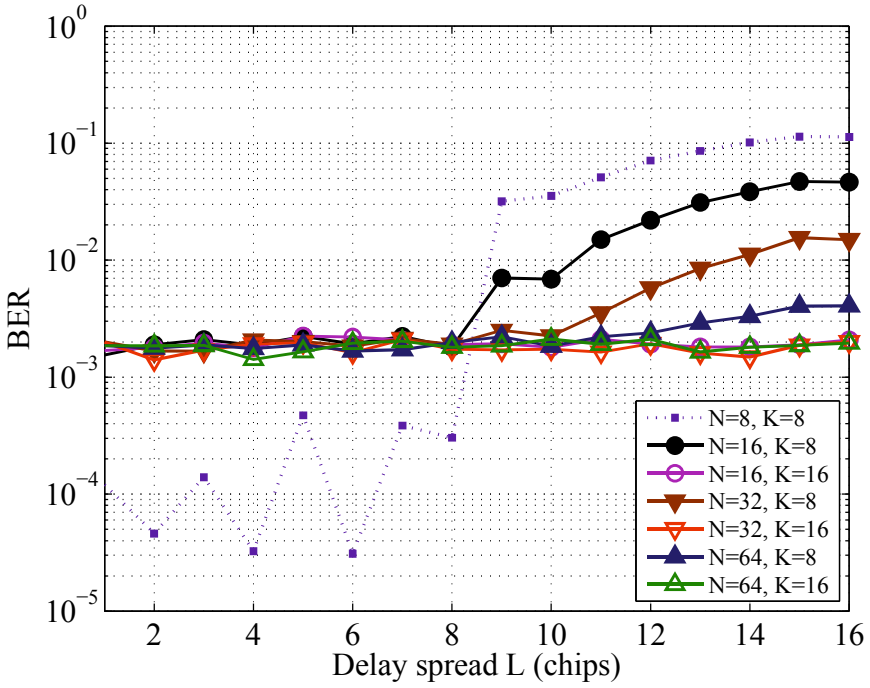

Figure 5.6: BER performance of BC-MC-ZCZ-CDMA with QPSK in delay spread L

It may be depend on use of an ideal pilot signal without noise, and ZCZ code of short length code length N.

Figure 5.7 shows the BER performance of BC-MC-ZCZ-CDMA with 16QAM over a two-path equal power delay profile with $L = 4$ and 9 for N and K. It is shown that the BER performance of proposed scheme with code length $N = 16, 32$ and 64 is almost the same for $L \leq K$. It is confirmed that the BER performance of the proposed scheme with code length $N = 8$ is improved approximately 6 dB for $BER = 10^{-4}$ in comparison with $N = 16, 32$ and 64. Moreover, for $L \leq K$, the BER performance is almost the same. However, for $L > K$, the BER performance is drastically decreased. It is seen that the BER performance of BC-MC-ZCZ-CDMA with 16QAM shows about 3 dB penalty compared with QPSK.

Figure 5.8 shows the BER versus delay spread L for $E_b/N_0 = 12$ dB in BC-MC-ZCZ-CDMA with 16QAM . It is clarified that the delay spread L does not affect the system performance if L does not exceed K. The capability of fighting against interference improves as code length N increases when delay spread L exceeds block

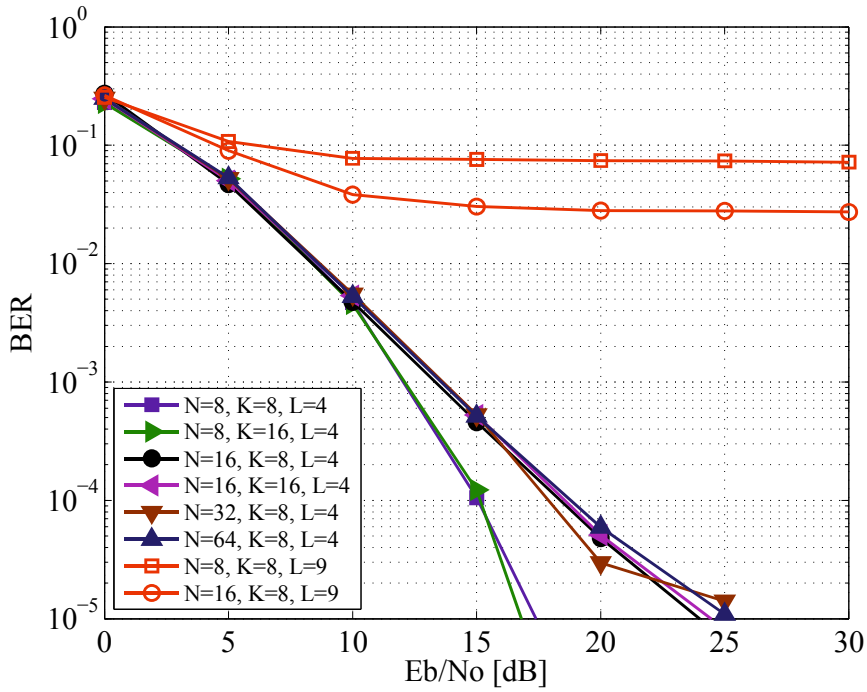

Figure 5.7: BER performance of BC-MC-ZCZ-CDMA with 16QAM for N and K

size K. For code length $N = 8$, the graph of BER for length of delay chips fluctuates. It may be depend on use of an ideal pilot signal without noise, and ZCZ code of short length code length N. It is seen that the BER performance of BC-MC-ZCZ-CDMA with 16QAM shows about 3 dB penalty compared with QPSK.

Fig.5.9 shows the BER performance of BC-MC-ZCZ-CDMA with frequency domain equalization, which is generally used for multicarrier communications to mitigate interferences and without one over a two-path equal power delay profile with delay spread $L = 4$ chips for multiple access with $M = 4$ users. It can be confirmed that those performance is the same.

Figure 5.10 shows the BER performance of BC-MC-ZCZ-CDMA and BC-DS-ZCZ-CDMA using ZCZ code $A(32, 16, 1)$ with QPSK for multiple access with $M = 4$ users. It is observed that the BER performance of the proposed scheme is better than that of the conventional scheme for the maximum delay chips L. Furthermore, the performance of the proposed scheme is maintained even if delay spread L increases. In this simulation, these frequency bands are almost the same since a filter is not considered, that is ideal.

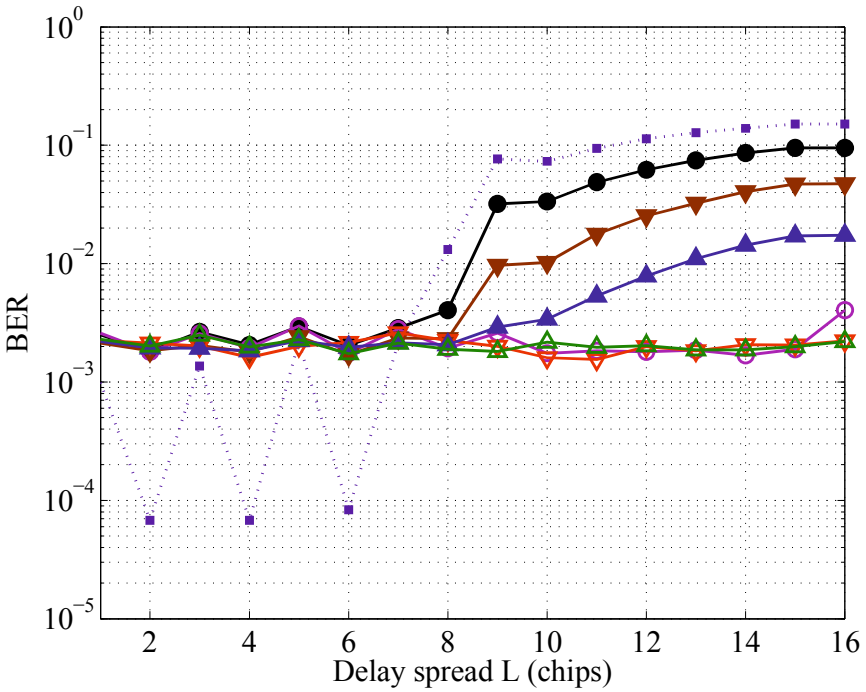

Figure 5.8: BER performance of BC-MC-ZCZ-CDMA with 16QAM in delay spread

Figure 5.11 shows the BER performance of BC-DS-ZCZ-CDMA using ZCZ code $A(32, 16, 1)$ with QPSK for multiple access with $M = 4$ users. It is observed that the BER performance of the conventional scheme is gradually decreased as the length of block size K increases. Although the MAI is free in BC-DS-ZCZ-CDMA, but the ISI caused by both multipath and large block size K induces system performance degradation. That is the reason that the conventional single carrier BC-DS-ZCZ-CDMA can not be applicable for high data rate transmission.

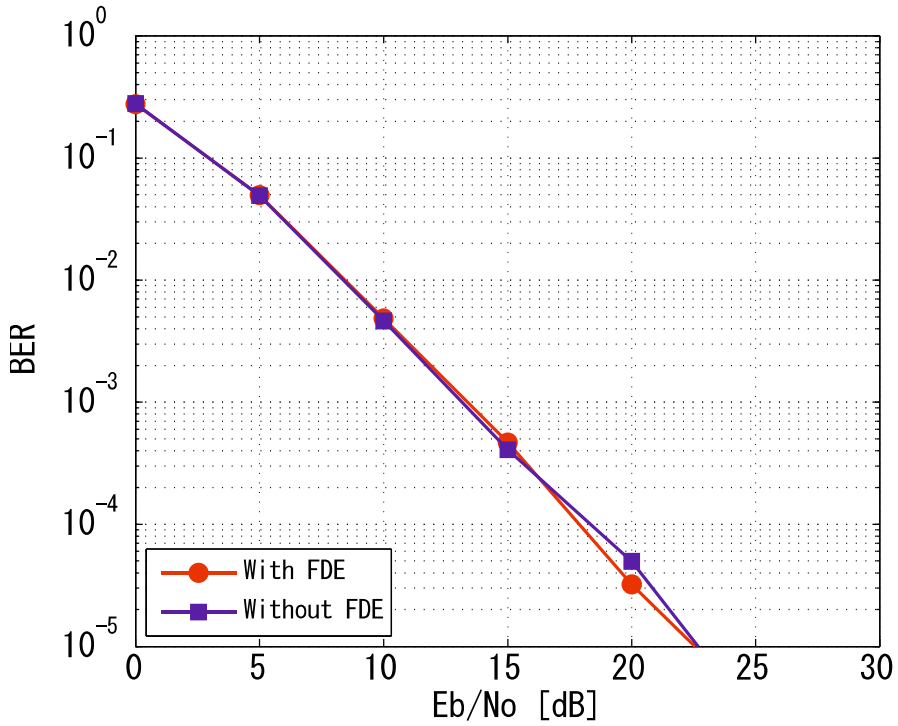

Figure 5.9: BER performance of BC-MC-ZCZ-CDMA in frequency domain equalization.

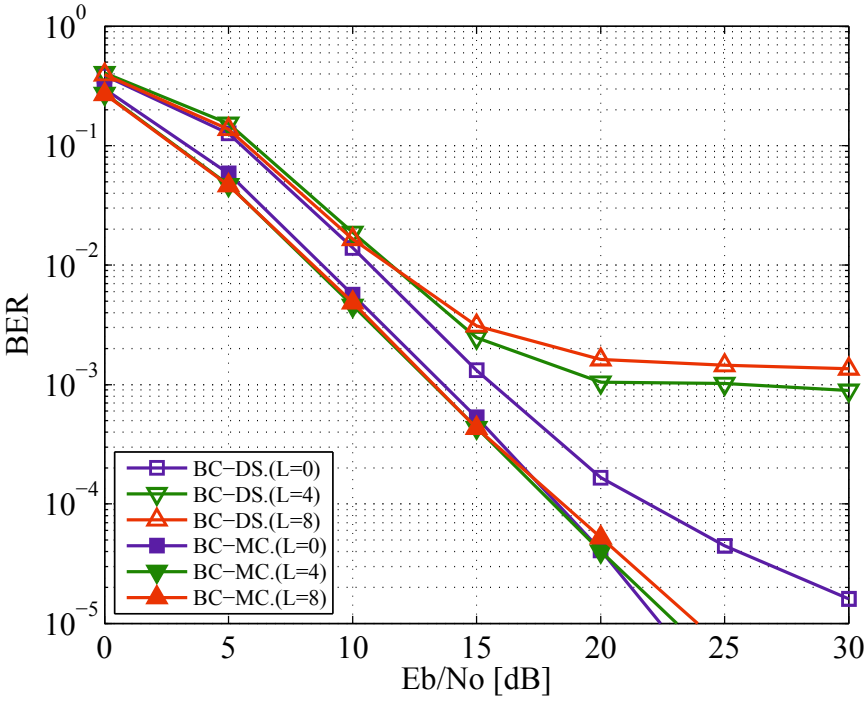

Figure 5.10: BER performance of BC-DS-ZCZ-CDMA and BC-MC-ZCZ-CDMA with QPSK in large delay spread ($M = 4$, $N = 32$, $K = 16$)

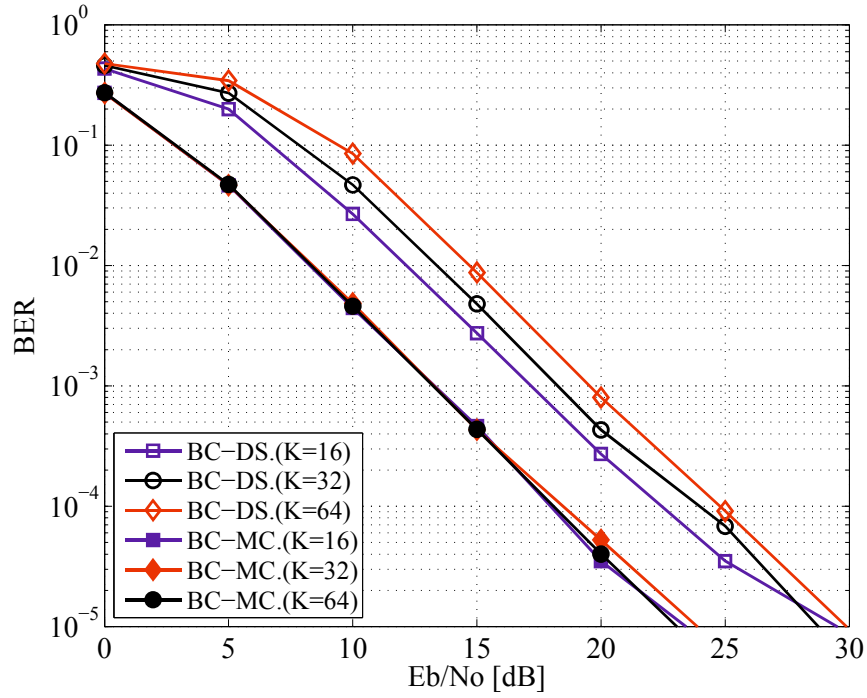

Figure 5.11: BER performance of BC-DS-ZCZ-CDMA with QPSK for K

Chapter6

Conclusions

This dissertation has proposed a novel multicarrier CDMA scheme with interference free performance using ZCZ code called BC-MC-ZCZ-CDMA in high data rate transmission with large delay spread. It has been confirmed that a considerable improvement was achieved with the proposed scheme.

In this chapter, the results derived in this dissertation are summarized and concluded in detail, and topics for further studies and future hopes are given.

6.1 Conclusions

After giving a brief introduction to the background and purpose of the research in chapter 1, some necessary fundamental knowledge was presented to help understand the main intention of the research in chapter 2. Firstly, the basic structure of the wireless communications was introduced, and the affects of multipath with large delay spread in real communication were shown. Next, different modulation schemes were introduced, and their BER performance over AWGN and fading channels was evaluated. As a result, the BER performance of BPSK and QPSK are same, and the BER of 16QAM worse than BPSK and QPSK in both channels. Finally, an intensive explanation was given to singlecarrier and multicarrier CDMA schemes. By comparison, the MC-CDMA is an more effective scheme for high data rate transmission than DS-CDMA, since the former has robustness to fading channel and the latter only limited in short-range communication.

In chapter 3, the ZCZ code and MC-CDMA using ZCZ with low correlation properties were investigated. Firstly, introduction of ZCZ was given and its orthogonality in Fourier transform was mathematically verified and clarified for one chip delay. Next, a singlecarrier BC-DS-ZCZ-CDMA scheme, based on block coding technique and DS-ZCZ-CDMA was presented, and its BER performance was evaluated in large delay spread. As a result, it is confirmed that although the MAI can be completely removed, but the ISI still exits. Finally, MC-ZCZ-CDMA without GI technique was introduced, and its BER performance was evaluated. As a result, by using the correlation properties and constructions of ZCZ code, these interference can be effectively removed. However, the the family size of ZCZ code for multiple users will be decreased.

In order to solve above problems, this dissertation has proposed a novel BC-MC-ZCZ-CDMA scheme based on the MC-ZCZ-CDMA with 2 chips GI in large delay spread. The proposed scheme was characterized by use of a block coding technique to remove MAI and ICI, and the MMSE Rake receiver with a pilot-symbol-aided channel estimation to utilize a delay wave and to reduce ISI. As a result, it has been clarified that proposed scheme possesses good BER performance for large delay spread dose not exceed the block size ($L \leq K$). The block size K does not almost affect the system performance if K is longer than the length of large delay spread L. However, the computational complexity increases as K increases, since the inverse matrix computation is performed. It has been also shown that ZCZ code $A(8, 4, 1)$ is effective. If code length N is large, the performance can be almost maintained, even if $L > K$. To cope with the change of a communication channel, length of a transmission packet may be shorten to utilize the Rake receiver without frequency domain equalization. Obviously, the proposed scheme can achieve good performance and high bandwidth efficiency over a multipath Rayleigh fading channel, and can be efficient multicarrier and multiple access scheme for future high data-rate wireless communications.

Consequently, simplicity in understanding and comparing the system performance of the proposal and conventional schemes over a multipath fading channel with large delay spread, the final conclusion was given in Table 6.1.

Table 6.1: Performance comparison of CDMA schemes

	Merits	Advantages and disadvantages
DS-CDMA (Single-carrier)	· Applicable to synchronous or asynchronous · Uses orthogonal or PN codes with low correlation	· Applicable to middle-range communication · MAI increases as No. of users increases · A complex controlling technique is needed · Inapplicable to high date rate transmission
DS-ZCZ-CDMA (Single-carrier)	· Quasi-synchronous · ZCZ code (GI addition) · RAKE receiver	· Can remove MAI · Can effectively use delay waves, since MAI does not exit · Inapplicable to high date rate transmission
BC-DS-ZCZ-CDMA (Single-carrier)	· Quasi-synchronous · ZCZ code · Block coding (GI addition) · RAKE receiver	· Can remove MAI · Can effectively use delay waves, since MAI does not exit · Inapplicable to high date rate transmission · Performance decrease as block size increases
MC-CDMA (Multi-carrier)	· Synchronous communication · Uses orthogonal code · Fourier Transform technique · Frequency domain equalization	· High robustness to interferences or to multipath fading channel · Applicable to downlink transmission ·Weak in a large delay spread channel · Transceiver becomes complex
MC-ZCZ-CDMA (Multi-carrier)	· Synchronous communication or asynchronous · ZCZ code (Zcz is large) · Fourier transform technique · Frequency domain equalization	· Able to mitigate MAI · MAI appears even in one chip delay spread · When length of delay is long, the number of users becomes small · Transceiver becomes complex
BC-MC-ZCZ-CDMA (Multi-carrier)	· Quasi-synchronous · ZCZ code · Fourier Transform technique · Block coding (GI addition) · RAKE receiver	· Effective in various applications · MAI be removed even in large delay spread · A complex controlling technique is needed · Does not need frequency domain equalization · The system performance does not change even the block size increases However, computational complexity increases

6.2 Further Study

There are several topics that deserve to be future studied.

· By using a software at the digital part and a hardware at the analog part, examine the effectiveness of propose technique in real system.

· Discuss in the field of optical wireless communications.

· Its application for future wireless communications is considered, since the proposed technique has strong potential to cope with interference.

Acknowledgment

I would like to express my sincere appreciation and gratitude to my advisor Prof. Shinya Matsufuji of Graduate School of Science and Engineering, Yamaguchi University for his constant guidance, support, understanding, patience, and most importantly, for his friendship not only for me, but also for all of the members in his research group. His vast experience and nice nature has given me a very great learning experience during the course of this research.

I would like to express my gratitude to associate Prof. Takahiro Matsumoto of Graduate School of Science and Engineering, Yamaguchi University who is the subchairpersons of my dissertation committee for your valuable advice and comments on my research and the constant support throughout three years.

I would like to express my gratitude to assistant Prof. Yuta Ida of Graduate School of Science and Engineering, Yamaguchi University for your great indications, guidance and valuable advice throughout two years. Without your support, this work would not have been possible.

I would also like to express my thanks to my research group members past and present Information and Communication Laboratory, Yamaguchi University. I have learned so much from all of you, from figuring out what research is, to choosing a research agenda, to learning how to present my work. Your constructive criticism and collaboration have been tremendous assets throughout my Ph.D.

I would like to express my great thanks to my family for their great source of love and motivation always.

References

[1] M.K. Simon, J.K. Omura, R.A. Scholtz and B.K. Levitt, " Spread Spectrum Communications, " Computer Science Press, 1985.

[2] R.E. Ziemer, R.L. Peterson and R.L, Peterson, " Digital Communications and Spread Spectrum Systems, " Macmillan Publishing Company, 1985.

[3] R. Prasad, " CDMA for Wireless Personal Communication, " Norwood, Artech House, 1996.

[4] M.K. Simon and M.S. Alouini, "Digital Communication over Fading Channels," Wiley-IEEE Press, 2004.

[5] S. Hara and R. Prasad, " Overview of Multicarrier CDMA, " IEEE Communications Magazine, Vol. 35, No. 12, pp. 126-133, Dec. 1997.

[6] S. Hara and R. Prasad, "Design and Performance of Multicarrier CDMA System in Frequency-selective Rayleigh Fading Channels, " IEEE Trans. on Vehicular Technology, Vol. 48, No. 5, pp. 1584-1595, Sept. 1999.

[7] F. Adachi, M. Sawahashi and H. Suda, " Wideband DS-CDMA for Next Generation Mobile Communication Systems, " IEEE Communications Magazine, Vol. 36, No. 9, pp. 56-69, Sept. 1998.

[8] J. Korhonen, " Introduction to 3G Mobile Communications, " Norwood, Artech House, 2003.

[9] H. Habuchi , T. Takebayashi and T. Hasegawa, " Analysis of BER Performance of the Spread Spectrum Communication System with Constraint Spreading

Code, " IEICE Transactions on Fundamentals, Vol. 79-A, No. 12, pp. 2078-2080, Dec. 1996.

[10] X. Liu and L. Hanzo, " Accurate BER Analysis of Asynchronous DS-CDMA Systems in Rician Channels, " Proc. of IEEE VTC'06, pp. 25-28, Sept. 2006.

[11] M.R. Karim and Mohsen Sarraf, " W-CDMA and CDMA2000 for 3G Mobile Net-works, " McGraw-Hill Professional, 2002.

[12] H. Torii and M. Nakamura, " Inter-Cell Interference of Approximately Synchronized CDMA Systems in Asynchronous Condition, " IEICE Trans. Communications, Vol. E87-B, No. 5, pp. 1318-1327, May 2004.

[13] N. Suehiro, " A Signal Design Without Co-channel Interference for Approximately Synchronized CDMA Systems, " IEEE Journal on Selected Areas in Communications, Vol. 12, No.5, pp. 837-841, June 1994.

[14] L. Hao and P.Z. Fan, " Performance Evaluation for a New Quasi-synchronous CDMA System Employing Generalized Orthogonal Sequences, " IEICE Trans. Information and System, Vol. E86-D, No. 9, pp. 1513-1524, Sept. 2003.

[15] P.Z. Fan and M. Darnell, "Sequence Design for Communications Applications," Research Studies Press LTD, 1997.

[16] R. Nidhi and D. Veeranna, " Performance Analysis on Different Modulation Techniques of MIMO in Multipath Fading Channel, " IOSR Journal of Engineering, Vol. 2, No. 4, pp. 738-743, Apr. 2012.

[17] M.S. Raju, A. Ramesh and A. Chockalingam, " BER Analysis of QAM with Transmit Diversity in Rayleigh Fading Channels, " Proc. of IEEE GLOBECOM'03, Vol. 2, pp. 641-645, Dec. 2003.

[18] T.S. Rappaport, "Wireless Communications: Principles and Practice," Prentice Hall, 2001.

[19] S. Bernard, " Rayleigh Fading Channels in Mobile Digital Communication Systems PartI: Characterization, " IEEE Communications Magazine, Vol. 30, No. 7, pp. 90-100, July 1997.

[20] C. Xiao, Y.R. Zheng and C. Beaulieu, " Statistical Simulation Models for Rayleigh and Rician Fading, " Proc. of ICC'03, pp. 3524-3529, May 2003.

[21] K. Noriyoshi, L. Guo and N. Suehiro, " Novel Signal Separation Principle Based on DFT with Extended Frame Fourier Analysis, " IEICE Trans. Communications, Vol. E79-B, No. 2, pp. 182-190, Feb. 1996.

[22] J.C. Huang, S. Matsufuji, T. Matsumoto and N. Kuroyanagi, " A ZCZ-CDMA System with BFSK Modulation, " International Journal of Communication Systems, Vol. 25, No. 12, pp. 1620-1638, Dec. 2012.

[23] P.Z. Fan, N. Suehiro, N. Kuroyanagi and X.M. Deng, " A Class of Binary Sequences with Zero Correlation Zone, " Electronics Letters, Vol. 35, No. 10, pp. 777-779, May 1999.

[24] P.Z. Fan and L. Hao, " Generalized Orthogonal Sequences and Their Applications in Synchronous CDMA Systems, " IEICE Trans. Fundamentals, Vol. E83-A, No. 11, pp. 2054-2069, Nov. 2000.

[25] X.H. Tang, P.Z. Fan and S. Matsufuji, " Lower Bounds on the Maximum Correlation of Sequence Set with Low or Zero Correlation Zone, " Electronics Letters, Vol. 36, No. 6, pp. 551-552, Mar. 2000.

[26] K. Takatsukasa, S. Matsufuji and Y. Tanada, "Formalization of Binary Sequence Sets with Zero Correlation Zone, " IEICE Trans. on Communications, Vol. E87-A, No. 4, pp. 887-891, Apr. 2004.

[27] S. Matsufuji, N. Kuroyanagi, N. Suehiro and P.Z. Fan, "Two Types of Polyphase Sequence Sets for Approximately Synchronized CDMA Systems, " IEICE Trans. on Communications, Vol. E86-A, No. 1, pp. 229-234, Jan. 2003.

[28] A. Zemlianov and G.D. Veciana, " Capacity of Ad-hoc Wireless Networks with Infrastructure Support, " IEEE Journal on Selected Areas in Communications, Vol. 23, No. 3, pp. 657-667, Mar. 2005.

[29] M. Tomita, N. Kuroyanagi, K. Ohtake, N. Suehiro and S. Matsufuji, " A Multirate CDMA System with Block Spreading Schemes for Anti-interference and

High Frequency Efficiency," IEICE Technical Report, WBS, Vol. 106, No. 553, pp. 43-48, Feb. 2007.

[30] S. Matsufuji, T. Matsumoto, T. Matsuo and N. Kuroyanagi, " A ZCZ-CDMA System with High Tolerance to Frequency Selective Fading," Proc. of IWSDA'11, pp. 157-160, Oct. 2011.

[31] W. Yue, Z.B. Muhammud and P.C. Justin, " Iterative Successive Interference Cancellation for Quasi-synchronous Block Spread CDMA Based on the Orders of the Times of Arrival," EURASIP Journal on Advances in Signal Processing, Vol. 11, No. 9, pp. 1-12, Mar. 2011.

[32] G. Leus and M. Moonen, " MUI-free Receiver for a Shift-orthogonal Quasi-synchronous DS-CDMA System Based on Block Spreading in Frequency Selective Fading," Proc. of Int. Conf. ASSP'02, pp. 2497-2500, June 2000.

[33] S.L. Zhou, G.B. Giannakis and C.L. Martret, " Chip-interleaved Block-spread Code Division Multiple Access," IEICE Trans. on Communications, Vol. 50, No. 2, pp. 235-248, Feb. 2002.

[34] H. Cheng, S.C. Chan and Z.G. Zhang, " Robust Channel Estimation and Multiuser Detection for MC-CDMA Systems Under Narrowband Interference," Journal of Signal Processing Systems, Vol. 52, No. 2, pp. 165-180, Aug. 2008.

[35] N. Kabaoglu, " Expectation-maximization-based Joint Data Detection and Channel Estimation for a Cellular Multi-carrier Code Division Multiple Access Network Using Single-hop Relaying," International Journal of Communication Systems, Vol. 26, No. 4, pp. 449-464, Apr. 2013.

[36] T. Shono, T. Yamada, T. Kobayashi and I. Sasase,"Spreading Code Assignment for Multicarrier CDMA System Over Frequency Selective Fading Channels," IEICE Trans. on Communications, Vol. E87-B, No. 10, pp. 3734-3746, Dec. 2004.

[37] K. Takeda and F. Adachi, " Frequency-domain MMSE Channel Estimation for Frequency-domain Equalization of DS-CDMA Signals," IEICE Trans. on Communications, Vol. E90-B, No. 7, pp. 1746-1753, July 2007.

[38] I. Cosovic, M. Schnell and A. Springer, "Combined-equalization for Uplink MC-CDMA in Rayleigh Fading Channels," IEEE Trans. on Communications, Vol. 53, No. 10, pp. 1609-1614, Oct. 2005.

[39] Y.L. Chena and R. Sumit, " Performance of Frequency-time MMSE Equalizer for MC-CDMA Over a Multipath Fading Channel," Wireless Personal Communications, Vol. 18, No. 2, pp. 179-192, Aug. 2001.

[40] D. Motter, "Spreading Sequences for Uplink and Downlink MC-CDMA Systems: PAPR and MAI Minimization," IEEE Trans. on Communications, Vol. 13, No. 5, pp. 465-471, Sept. 2002.

[41] H. Steendam and M. Moeneclaey, " Comparison of the Sensitivities of MC-CDMA and MC-DS-CDMA to Carrier Frequency Offset," Symposium on Communications and Vehicular Technology, Proc. of SCVT-200, pp. 166-173, Oct. 2000.

[42] A. Abudoukeremu, Y. Ida, T. Matsumoto and S. Matsufuji, "Multicarrier Transmission Systems Using Orthogonal Spreading Sequences in Large Delay Spread Channel," Proc. of IWSDA'13, pp. 84-87, Oct. 2013.

[43] S.H. Tsai, Y.P. Lin and C.C.J. Kuo, " MAI-free MC-CDMA Systems Based on Hadamard-Walsh Codes," IEEE Trans. on Signal Processing, Vol. 54, No. 8, pp. 3166-3179, Aug. 2006.

[44] B. Choi and L. Hanzo, "Crest Factors of Complementary-sequence-based Multicode MC-CDMA Signals," IEEE Trans. on Wireless Communications, Vol. 2, No. 6, pp. 1114-1119, Nov. 2003.

[45] C. Zhang, X.M. Tao, S. Yamada and M. Hatori, " Sequence Set with Zero Correlation Zones and Its Application in MC-CDMA System," IEICE Trans. Fundamentals, Vol. E89-A, No. 9, pp. 2275-2282, Sept. 2006.

[46] X.M. Tao, C. Zhang and J.H. Lu, " Doppler Diversity in MC-CDMA Systems with T-ZCZ Sequences for Doppler Spread Cancellation," IEICE Trans. Fundamentals, Vol. E90-A, No. 11, pp. 2361-2368, Nov. 2007.

[47] D.J. Basilio, L.P. Linde and B.T. Maharaj, "Uplink MC-DS-CDMA Using ZCZ Sequences for Frequency Selective Block Fading Channel," IEEE AFRICON '09, pp. 1-6, Sept. 2009.

[48] N.S. Weerasinghe and T. Hashimoto, "CS-CDMA/CP with M-ZCZ Codes Over a Multipath Fading Channel with Excess Spreads," Proc. of ICC'07, pp. 2835-2840, June 2007.

[49] V.M.D. Silva and E.S. Sousa, "Multicarrier Orthogonal CDMA Signals For Quasi-synchronous Communication Systems," IEEE Journal on Selected Areas in Communications, Vol. 12, No. 5, pp. 842-845, June 1994.

[50] Golay and J.E. Marcel, "Complementary Series," Information Theory, IRE Transactions, Vol. 7, No. 2, pp. 82-87, Apr. 1961.

[51] T. Hayashida, S. Matsufuji, T. Matsumoto and P.Z. Fan, "Construction of ZCZ Codes with Low Aperiodic Autocorrelation," Journal of Signal Processing, Vol. 16, No. 6, pp. 477-485, Nov. 2012.

[52] S. Matsufuji, T. Matsumoto and K. Fanakoshi, "Properties of Even-shift Orthogonal Sequences," Proc. of IWSDA'07, pp. 181-184, Sept. 2007.

[53] S. Matsufuji and N. Suehiro, "Functions for Even-shift Orthogonal Sequences," Technical Report of IEICE, Vol. 96, No. 427, pp. 25-30, Dec. 1996.

[54] T. Hayashi, "Binary Sequences with Orthogonal Subsequences and Zero Correlation Zone," IEICE Trans. Fundamentals, Vol. E85-A, No. 6, pp. 1420-1425, June 2002.

[55] A. Abudoukeremu, Y. Ida, T. Matsumoto and S. Matsufuji, "On Block Coding MC-ZCZ-CDMA System," Proc. of SITA'13, pp. 285-288, Nov. 2013.

[56] A. Abudoukeremu, S. Matsufuji, Y. Ida and T. Matsumoto, "A Novel Multicarrier CDMA Scheme with Interference Free Performance in Very Large Delay Spread," ITE Transaction on Media Technology and Applications, 2014 (to be published).

[57] R.N. Van and R. Prasad, " OFDM for Wireless Multimedia Communications, " Norwood, Artech House, 2000.

[58] C. Ahn, D. Har, T. Omor and K. Hashimoto, " Frequency Symbol Spreading Based Adaptive Subcarrier Block Selection for OFDMA System," Digital Signal Processing, Vol. 22, No. 3, pp. 518-525, May 2012.

[59] Y. Ida, C.J. Ahn, T. Kamio, H. Fujisaka and K. Haeiwa, " An Interference Cancellation Scheme for TFI-OFDM in Time-variant Large Delay Spread Channel," Radioengineering, Vol. 18, No. 1, pp. 75-82, April 2009.

[60] E.A. Sourour and M. Nakagawa, " Performance of Orthogonal Multicarrier CDMA in a Multipath Fading Channel, " IEEE Trans. on Communications, Vol. 44, No. 3, pp. 356-367, Mar. 1996.

[61] T. Sao and F. Adachi, " Comparative Study of Various Frequency Equalization Techniques for Downlink of a Wireless OFDM-CDMA System, " IEICE Trans. on Communications, Vol. E86-B, No. 1, pp. 352-364, Jan. 2003.